



Published in final edited form as:

Mol Cell Endocrinol. 2021 October 01; 536: 111400. doi:10.1016/j.mce.2021.111400.

IGFBP-1 hyperphosphorylation in response to nutrient deprivation is mediated by activation of protein kinase C α (PKC α)

Allan W. Chen^a, Kyle Biggar^{b,1}, Karen Nygard^{c,1}, Sahil Singal^a, Tiffany Zhao^a, Cun Li^{d,e}, Peter W. Nathanielsz^{d,e}, Thomas Jansson^{f,**}, Madhulika B. Gupta^{a,g,h,*}

^aDepartment of Biochemistry, University of Western Ontario, London, ON, Canada

^bInstitute of Biochemistry, Carleton University, Ottawa, ON, Canada

^cBiotron Integrated Microscopy Facility, University of Western Ontario, London, ON, Canada

^dUniversity of Wyoming, Laramie, WY, USA

^eSouthwest National Primate Research Center, San Antonio, TX, USA

^fDepartment of Obstetrics and Gynecology, Division of Reproductive Sciences, University of Colorado Anschutz Medical Campus, Aurora, CO, USA

^gDepartment of Pediatrics, University of Western Ontario, London, ON, Canada

^hChildren's Health Research Institute, London, ON, Canada

Abstract

Fetal growth restriction (FGR) is associated with decreased nutrient availability and reduced insulin-like growth factor (IGF)-I bioavailability via increased IGF binding protein (IGFBP)-1 phosphorylation. While protein kinase C (PKC) is implicated in IGFBP-1 hyperphosphorylation in nutrient deprivation, the mechanisms remain unclear. We hypothesised that the interaction of PKC α with protein kinase CK2 β and activation of PKC α under leucine deprivation (L0) mediate fetal hepatic IGFBP-1 hyperphosphorylation. Parallel Reaction Monitoring Mass Spectrometry (PRM-MS) followed by PKC α knockdown demonstrated the PKC α isoform interacts with IGFBP-1 and CK2 β under L0. Pharmacological PKC α activation with phorbol 12-myristate

*Corresponding author. Departments of Pediatrics and Biochemistry, University of Western Ontario and Children's Health Research Institute, VRL Room A5-136 (WC), 800 Commissioners Road East, London, ON, N6C 2V5, Canada. **Corresponding author. mbgupta@uwo.ca (M.B. Gupta).

¹Equal contributions.

CRediT authorship contribution statement

Allan W. Chen: Conceptualization, Methodology, Investigation, Writing – original draft, preparation, Writing – review & editing. **Kyle Biggar:** Investigation, Data curation, Writing – review & editing. **Karen Nygard:** Investigation, Methodology, Data curation, Writing – review & editing. **Sahil Singal:** Investigation. **Tiffany Zhao:** Investigation. **Cun Li:** Methodology, Writing – review & editing. **Peter W. Nathanielsz:** Methodology, Writing – review & editing, Funding acquisition. **Thomas Jansson:** Methodology, Writing – review & editing, Funding acquisition. **Madhulika B. Gupta:** Conceptualization, Methodology, Writing – original draft, preparation, Writing – review & editing, Funding acquisition.

Declaration of competing interest

The authors report no conflicts of interest related to this work.

Appendix A. Supplementary data

Supplementary data to this article can be found online at <https://doi.org/10.1016/j.mce.2021.111400>.

13-acetate (PMA) increased whereas inhibition with bisindolylmaleimide II (Bis II) decreased IGFBP-1 phosphorylation (Ser101/119/169, Ser98 + 101 and Ser169 + 174), respectively. Furthermore, PMA mimicked L0-induced PKC α translocation and IGFBP-1 expression. PKC α expression was increased in baboon fetal liver in FGR, providing biological relevance *in vivo*. In summary, we report a novel nutrient-sensitive mechanism for PKC α in mediating IGFBP-1 hyperphosphorylation in FGR.

Keywords

Fetal growth restriction; Placental insufficiency; Protein interaction; Protein kinase CK2; Baboon

1. Introduction

Insulin-like growth factor I (IGF-I) is a key regulator of fetal growth (Liu et al., 1993; Murphy et al., 2006). IGF binding protein 1 (IGFBP-1) is mainly secreted by fetal liver (Han et al., 1996) and is a major regulator of IGF-I bioactivity in fetal life, decreasing the bioavailability of the growth factor when bound to the IGF binding protein (Chard, 1994). Increased phosphorylation of IGFBP-1 increases its affinity for IGF-I (Jones et al., 1993a) and potently inhibits IGF-I dependent cellular functions such as cell proliferation, amino acid transport (Yu et al., 1998) as well as DNA synthesis (Koistinen et al., 1993) compared to the non-phosphorylated form.

We have previously shown that the predominant increase in binding affinity of IGFBP-1 for IGF-1 is due to an increase in the abundance of specific IGFBP-1 phosphoisoforms (site and degree of phosphorylation) rather than increases in total IGFBP-1 or even total phospho-IGFBP-1 (Seferovic et al., 2009). Furthermore, the functional effects of IGFBP-1 phosphorylation on IGF-I bioavailability and action are highly dependent on the specific residues that are phosphorylated and the degree of phosphorylation (Abu Shehab et al., 2013). Phosphorylation has been reported to increase IGFBP-1 stability by increasing its resistance to proteolysis (Gibson et al., 2001) thereby further sequestering IGF-I and inhibiting IGF-I function more potently.

The major site of IGFBP-1 phosphorylation has been identified as Ser101 with a 3-fold reduction observed in IGF-I binding affinity following phosphorylation at this site (Jones et al., 1993a). We (Seferovic et al., 2009; Abu Shehab et al., 2010) and others (Jones et al., 1993b) identified IGFBP-1 phosphorylation at Ser95, Ser98, and Ser119 in addition to Ser101 within the mid-linker region along with Ser169 and Ser174 in the C-terminal domain (Abu Shehab et al., 2013). Apart from Ser95 and Ser174, all other residues have been demonstrated to elicit varied increases in IGF-I affinity and inhibition of type 1 IGF receptor (IGF-IR) activation (Abu Shehab et al., 2013). The effects of phosphorylation at Ser119 remained similar to Ser101 (Jones et al., 1993a; Abu Shehab et al., 2013). We also demonstrated that leucine deprivation (L0) profoundly increased IGFBP-1 phosphorylation at a discrete site (Ser119) which enhanced IGF-I affinity (~30x) and inhibited IGF-I stimulated cell proliferation (Seferovic et al., 2009).

Fetal growth is determined by many disparate influences, including uteroplacental environment, oxygen and nutrient availability (Murphy et al., 2006). FGR due to placental insufficiency can be defined as a condition of impaired placental nutrient and oxygen transfer. Decreased circulating levels of essential amino acids, such as leucine, are common in growth restricted fetuses (Cetin et al., 1988, 1990). IGFBP-1 is a major regulator of IGF action in catabolic states such as malnutrition (Matsukawa et al., 2001) and hypoxia (Tazuke et al., 1998; Popovici et al., 2001) during which IGFBP-1 is hyperphosphorylated (Seferovic et al., 2009; Abu Shehab et al., 2014; Damerill et al., 2016) and potentially sequesters IGF-I, subsequently inhibiting IGF-I function (Seferovic et al., 2009; Abu Shehab et al., 2013). Additionally, decreased nutrient availability due to maternal nutrient restriction (MNR) increases the expression and phosphorylation of IGFBP-1 in the liver of baboon fetus *in vivo*, suggesting an important biological role of IGFBP-1 phosphorylation in restricting fetal growth (Abu Shehab et al., 2014). It has been shown that depletion of all essential amino acids or leucine *in vitro* alone is sufficient to induce IGFBP-1 expression (Straus et al., 1993; Jousse et al., 1998) and phosphorylation (Seferovic et al., 2009; Malkani et al., 2015, 2016). Limited data, however, is available to identify and define the actions of the kinases controlling IGFBP-1 phosphorylation in L0.

Based on amino acid sequences conserved in all six IGF binding proteins (IGFBPs), protein kinase CK2, protein kinase A (PKA) and protein kinase C (PKC) are candidate kinases mediating IGFBP-1 phosphorylation (Ankrapp et al., 1996; Coverley and Baxter, 1997). The CK2 consensus sequence (Meggio and Pinna, 2003) conforms to Ser101, Ser119 and Ser169 (Abu Shehab et al., 2010) which are involved in IGF-I binding (Abu Shehab et al., 2010). In our previous work using HepG2 cells, we demonstrated an IGFBP-1 and CK2 interaction which was induced by hypoxia and mediated by an mTOR and CK2 interaction (Singal et al., 2018). These findings were consistent in MNR baboon fetal liver tissue *in vivo* which demonstrated increased CK2 activity and IGFBP-1 hyperphosphorylation correlated with mTOR inhibition (Abu Shehab et al., 2014). Furthermore, we demonstrated the regulation of IGFBP-1 phosphorylation at Ser101, Ser119 and Ser169 in L0 by CK2 where PKC played a key supporting role (Malkani et al., 2016). The PKC family consists of multiple isoforms (Liu and Heckman, 1998; Webb et al., 2000). Importantly, PKC isoforms in different tissues and cell types are differentially regulated by nutrient availability. For example, leucine activates PKC in skeletal muscle (Vary et al., 2005) and chicken hepatocytes (Lee et al., 2008) while low protein diets have been shown to inhibit PKC activity in pancreatic islets (Lippo BR da et al., 2015). Alternatively, amino acid deprivation induces PKC η expression in MCF-7 cells (Raveh-Amit et al., 2009). A role for PKC in regulating IGFBP-1 expression has been suggested in HepG2 cells (Lee et al., 1992) and in human endometrial carcinoma cells (Gong et al., 1992) but a role for PKC in IGFBP-1 phosphorylation in response to L0 has not yet been demonstrated. Three PKC isoforms, PKC α , PKC β and PKC ζ are reported to regulate CK2 activity in HCT116 and HEK293 cells by directly phosphorylating CK2 α at Ser194 and Ser277 (Lee et al., 2016). Whether PKC contributes to IGFBP-1 hyperphosphorylation in response to L0 by interacting with CK2 remains unknown.

Functionally, PKC is activated via phosphorylation which ultimately mediates mechanisms such as protein-protein interactions, subcellular targeting and PKC translocation to membrane compartments (Steinberg, 2008). Activation of conventional PKC isoforms

(cPKCs) has been reported by conserved autophosphorylation of PKC at Thr250 (Ng et al., 1999). Moreover, increased PKC α expression has been observed in a rat model of FGR (Langdown et al., 2001). Whether any specific PKC isoform(s) plays a role in fetal hepatic IGFBP-1 phosphorylation remains to be determined.

Using HepG2 cells as a well-established model for human fetal hepatocytes (Kelly and Darlington, 1989; Wilkening et al., 2003), we tested the hypothesis that interaction of PKC α with CK2 β and activation of PKC α via its translocation to a membrane compartment under L0 mediates fetal hepatic IGFBP-1 hyperphosphorylation. We used fetal liver of a well-established baboon model of MNR to determine the translational relevance of the study.

2. Results

2.1. IGFBP-1, CK2 β , and PKC α reciprocally co-immunoprecipitate

To identify the involvement of PKC in IGFBP-1 phosphorylation under L0 we first performed simultaneous co-immunoprecipitations (co-IPs) of IGFBP-1, CK2 β , and Pan-PKC (recognizes the conserved activation-loop of PKC isoforms) in HepG2 cells cultured with (L450) or without (L0). We performed western blot analysis to detect IGFBP-1, PKC α and CK2 β in L450 and L0 co-IPs (Fig. 1). We demonstrate that PKC α co-IPs IGFBP-1 in L0 and that PKC α fails to co-IP IGFBP-1 in L450 (Fig. 1A). Similarly, PKC α also reciprocally co-IPs CK2 β which occurs only in L0 conditions (Fig. 1B). However, IGFBP-1 and CK2 β reciprocally co-IP both in L450 and L0 (Fig. 1C). These data demonstrate that although IGFBP-1 is associated with CK2 β in both L450 and L0, PKC α only co-IPs with IGFBP-1 and/or CK2 β specifically in L0. These findings provide convincing evidence that PKC α is a nutritionally sensitive kinase responding to L0 conditions resulting in enhanced protein-protein interactions with both IGFBP-1 and CK2 β . Furthermore, IP with rabbit preimmune IgG used as a negative control failed to immunoprecipitate IGFBP-1, CK2 β or PKC α supporting the rigor of our approach.

In order to identify and confirm the PKC isoform which co-IPs with IGFBP-1 or with CK2 β in L0, we performed PRM-MS analysis. PRM-MS detected fifteen PKC specific peptides from the respective IGFBP-1 and CK2 β IPs collected from L0 cultured HepG2 cell lysates (Fig. 2). Three out of 15 detected PKC specific peptides were homologous peptides unique to conventional PKC isoforms while 12 of 15 were unique solely to PKC α (Table 1). Each detected PKC peptide spawned at least four daughter ions with co-detection of the parent immunoprecipitating protein indicating robust detection (Fig. 2B-D). IGFBP-1 peptides were co-detected from both IGFBP-1 and CK2 β IPs with specific detection of peptides containing IGFBP-1 phosphorylation sites Ser98, Ser101, Ser119 and Ser169 with the Ser119 peptide being detected with the highest intensity (Fig. 2E). Our targeted MS approach corroborates Western blot findings (Fig. 1); IGFBP-1 co-IPs CK2 β and PKC α ; CK2 β co-IPs IGFBP-1; and PKC α , and Pan-PKC co-IPs IGFBP-1 and CK2 β in L0. PRM-MS data provide strong evidence that the PKC isoform involved in L0 is PKC α as the specific interacting PKC α isoform with CK2 and IGFBP-1 in L0.

2.2. PKC α siRNA silencing reduces IGFBP-1 phosphorylation

To confirm the mechanistic involvement of PKC α in mediating IGFBP-1 phosphorylation in L0, we silenced the PKC α isoform in HepG2 cells cultured with and without leucine. PKC α siRNA reduced PKC α expression in both L450 and L0 conditions with high efficiency (-71% ($p = 0.0003$) and -70% ($p = <0.0001$) respectively) (Supplemental Figure 1). PKC α knockdown reduced total IGFBP-1 secretion by -51% ($p = 0.015$) in L450 and -36% ($p = 0.0428$) in L0 compared to their respective scramble siRNA controls. Further PKC α knockdown prevented L0-mediated induction of total IGFBP-1 secretion which was reduced to levels comparable to scramble siRNA transfected L450 treatment (-1% , $p = 0.96$) (Fig. 3A).

PKC α knockdown affected all three IGFBP-1 phosphorylation sites (Fig. 3B-D) both with and without leucine. In L450, PKC α knockdown reduced pSer101 by -78% ($p = 0.0035$), pSer119 by -67% ($p = 0.0106$) and pSer169 by -75% ($p = 0.0193$). In L0, PKC α knockdown also reduced pSer101 by -56% ($p = 0.0014$), pSer119 by -39% ($p = 0.005$) and pSer169 by -39% ($p = 0.0086$).

Furthermore, PKC α knockdown reduced L0 mediated induction of IGFBP-1 at pSer101 (-37% , $p = 0.0309$) and IGFBP-1 pSer119 (-21% , $p = 0.0447$) compared to L450 transfected with scrambled siRNA (Fig. 3B and C). Overall, these data suggest that the PKC α is involved in mediating both the increased total IGFBP-1 secretion and the IGFBP-1 hyperphosphorylation in response to L0.

2.3. Immunofluorescence staining and proximity ligation assay indicate PKC α + IGFBP-1 and PKC α + CK2 β interactions are induced by leucine deprivation

We performed dual immunofluorescence (IF) to investigate cellular staining as an additional alternative approach to investigate potential interactions between PKC α +IGFBP-1 (Fig. 4). Dual IF of PKC α +IGFBP-1 (Fig. 4A) demonstrates mostly cytosolic PKC α (Fig. 4A; i, v) and IGFBP-1 (Fig. 4A; ii, vi) staining with more pronounced perinuclear IGFBP-1 staining in L0. Merged channel images (Fig. 4A; iii, vii) of PKC α +IGFBP-1 demonstrate greater yellow fluorescence, indicating an increased overlap between PKC α and IGFBP-1 fluorescence signals suggesting increased co-localization between PKC α and IGFBP-1 as compared to L450 conditions.

We employed the highly sensitive and specific *in situ* proximity ligation assay (PLA) complementary to dual IF for PKC α +IGFBP-1 (Fig. 4B). Within HepG2 cells cultured in L450, limited PLA signals were observed (Fig. 4B; a). PLA signals between PKC α +IGFBP-1 were induced by L0 (Fig. 4B; b). L0 significantly increased PKC α +IGFBP-1 proximity reactions by $+193\%$ ($p < 0.0001$) (Fig. 4B; d).

We then investigated a potential PKC α +CK2 β interaction in L0 utilizing similar dual IF staining which demonstrated strong co-localization of PKC α +CK2 β in L450 and L0 (Fig. 5A). Furthermore, PLA demonstrated an abundance of proximity signals between PKC α +CK2 β in L450 (Fig. 5B; a) and L0 (Fig. 5B; b). Automated quantification of PLA signals demonstrated a modest increase in PLA signals derived from PKC α and CK2 β proximity signals in L0 compared to L450 ($+24\%$, $p = 0.0293$) (Fig. 5B; d). Considering we

failed to detect co-IP of PKC α and CK2 β in L450 (Fig. 1B), the abundance of proximity reactions between PKC α +CK2 β in L450 (Fig. 5B; a) may be due to the ubiquitous nature of both proteins (Webb et al., 2000; Litchfield, 2003). However, successful co-IP of PKC α and CK2 β and the increase of PKC α +CK2 β PLA signals in L0 indicate that a limitation in leucine availability induces a PKC α +CK2 β interaction. Overall, PLA indicates close proximity and potentially increased interactions of both PKC α +IGFBP-1 and PKC α +CK2 β in HepG2 cells cultured under L0.

Furthermore, we previously found that IGFBP-1+CK2 β interactions were induced by hypoxia in HepG2 cells (Singal et al., 2018). Here, we examined IGFBP-1+CK2 β interactions in L0 (Fig. 6) in HepG2 cells. Co-localization between IGFBP-1 and CK2 β were similarly induced by L0 (Fig. 6A). Complementary PLA demonstrated an +60% increase ($p = 0.0131$) in IGFBP-1+CK2 β proximity reactions (Fig. 6B; d).

2.4. Pharmacological inhibition and activation of PKC demonstrates that PKC mediates IGFBP-1 phosphorylation

Next, we investigated whether PKC inhibition with Bis II and activation with PMA in HepG2 cells cultured with and without leucine alter phosphorylation of IGFBP-1 (Fig. 7). While total IGFBP-1 secretion in cell media (CM) was increased in response to L0 (+162%, $p = 0.014$), PKC inhibition by Bis II reduced L0 mediated increases in IGFBP-1 secretion (-57%, $p = 0.02$). Bis II also reduced total IGFBP-1 secretion in L450 (-86%, $p = 0.0004$). On the other hand, induction of PKC by PMA enhanced total IGFBP-1 secretion both in L0 (+912%, $p = 0.0013$) and in L450 (+649%, $p = 0.016$) (Fig. 7A).

The effects of Bis II and PMA were also tested on phosphorylation of IGFBP-1. Phosphorylation at all three IGFBP-1 sites were significantly induced in response to L0 (pSer101 +376%, $p = 0.009$; pSer119 +110%, $p = 0.033$; pSer169 +404%, $p = 0.008$). Bis II treatment largely prevented IGFBP-1 phosphorylation induced by L0 (pSer101 -78%, $p = 0.009$; pSer119 -66%, $p = 0.017$; pSer169 -89%, $p = 0.0073$) (Fig. 7B-D), resulting in no significant difference between IGFBP-1 phosphorylation in L450 and L0 with Bis II. PKC inhibition by Bis II in L450 reduced IGFBP-1 phosphorylation (pSer101 -80%, $p = 0.008$; pSer119 -77%, $p = 0.01$; pSer169 -78%, $p = 0.002$).

PMA induced IGFBP-1 phosphorylation in L0 at pSer101 and pSer169 (pSer101 +443%, $p = 0.03$; and pSer169 +311%) but to a lesser extent than observed in L450 (pSer101 +1013%, $p = 0.02$; pSer119 +121%, $p = 0.016$; pSer169 +1644%, $p = 0.0131$) (Fig. 7B, D). However, PKC induction by PMA in L0 did not induce IGFBP-1 phosphorylation at pSer119 (+11%, $p = 0.58$) (Fig. 7C). Overall, these data led us to conclude that PKC inhibition leads to reduced IGFBP-1 and secretion and phosphorylation while PKC activation increases both IGFBP-1 secretion and phosphorylation, providing strong evidence for a key role of PKC α in IGFBP-1 phosphorylation and secretion in HepG2 cells. Furthermore, PKC inhibition prevented L0-induced IGFBP-1 phosphorylation and secretion and L0 prevented PMA induced IGFBP-1 phosphorylation specifically at Ser119 (+11%, $p = 0.58$) indicating that PKC mediates L0 induced IGFBP-1 phosphorylation particularly at Ser119 which is consistent with our previous findings (Seferovic et al., 2009). We further utilized heat map analysis derived from PRM-MS data to gain a visual overview and demonstrate

that PKC contributes to IGFBP-1 phosphorylation at specific dual sites. HepG2 cells treated with Bis II, PMA and 4,5,6,7-tetrabromobenzotriazole (TBB), an ATP site selective inhibitor of CK2 singly and in combination clearly demonstrated the respective expected changes in phosphorylation sites in response to kinase inhibition and activation (Fig. 8). We performed dual phosphorylation site analysis of IGFBP-1 at Ser169+Ser174 (Fig. 8A) and at Ser98+Ser101 (Fig. 8B) within targeted doubly phosphorylated peptides identified in relation to their relative retention time of an IGFBP-1 internal peptide.

The changes detected in both dually phosphorylated peptides in response to inhibitor and activator treatments were similar to changes in phosphorylation at Ser101, Ser119 and Ser169 as determined by Western blotting (Fig. 7). In brief, PKC inhibition and activation with Bis II and PMA universally reduced and induced IGFBP-1 phosphorylation at Ser169+174 and Ser98+101, respectively. Treatment with Bis II + PMA expectedly minimized the induction of IGFBP-1 phosphorylation by PMA treatment. CK2 inhibition with TBB (10 μ M) additionally reduced IGFBP-1 phosphorylation. TBB in conjunction with PMA reduced the effects of PMA alone on the induction of IGFBP-1 phosphorylation, suggesting that PKC and CK2 act in concert in mediating IGFBP-1 phosphorylation.

2.5. Leucine deprivation induces PKC α translocation concurrent with IGFBP-1 secretion in a time dependent manner

As we have established in this study that PKC α mediates both IGFBP-1 phosphorylation and secretion (Figs. 3, 7 and 8), we aimed to identify whether PKC α is specifically activated by L0. HepG2 cells were exposed to L0 (Fig. 9A) or PKC inducer PMA (Fig. 9B) in a time dependent manner (0 h, 6 h, 12 h) and were differentially fractionated for enrichment of cytosolic (supernatant) and membrane (pellet) fractions (Fig. 9A-B). Western blot demonstrated time dependent PKC α translocation to a membrane compartment (pellet) when cells were cultured under L0 (Fig. 9A). At 0 h and 6 h, the expression of PKC α was relatively more prominent in the supernatant fraction as compared to pellet fraction. PKC α membrane translocation was induced at 12 h where we observed an increase in PKC α in the pellet fraction and a decrease in PKC α in the supernatant fraction (Fig. 9A). Importantly, IGFBP-1 expression was highest at 12 h of L0 exposure, concomitant with translocation of PKC α . Treatment of cells in parallel with PMA (Fig. 9B) induced PKC α membrane translocation at 6 h which persisted at 12 h (Fig. 9B), showing a similar time course of PKC α translocation.

To obtain additional evidence for PKC α time dependent translocation as a novel mechanism in nutrient sensitive regulation of IGFBP-1, HepG2 cells exposed to L0 or PMA over the same time course were used to perform IF staining for PKC α (green) (Fig. 10). PKC α translocation to membrane compartments are shown by white arrows and occurred at 12 h of L0 exposure. PMA which mimicked L0 effects as detected by western blot analysis (Fig. 9B), induced a comparable degree of PKC α membrane translocation. These data corroborate western blot findings where we detected observable PKC α translocation at 12 h of L0 exposure and 6 h of PMA exposure.

2.6. IGF-1 bioactivity is altered by PKC α contributions to IGFBP-1 phosphorylation

Utilizing an IGF-1R autophosphorylation assay in P6 cells, we further demonstrated changes in IGFBP-1 phosphorylation by PMA treatment (Fig. 11A) and PKC α silencing (Fig. 11B) affecting the bioactivity of IGF-I. IGF-I binding to the IGF-1R results in the autophosphorylation of IGF-1R β (Tyr1135) which is an indicator of cell growth and proliferation (Girnit et al., 2014). IGF-I alone (+IGF-I, positive control) induced pIGF-1R^{Tyr1135} by +1050% ($p < 0.0001$) opposed to the absence of IGF-I (-IGF-I, negative control). Treatment with L450 and L0 media reduced pIGF-1R^{Tyr1135} by -55% ($p = 0.0014$) and -73% ($p < 0.0001$) against +IGF-I alone, respectively. A further -80% decrease ($p < 0.0001$) in IGF-1R autophosphorylation was observed with L450+PMA whilst L0+PMA produced a -88% decrease ($p < 0.0001$). Compared to L450, L0 reduced pIGF-1R^{Tyr1135} by -39% ($p = 0.0492$) while PMA reduced pIGF-1R^{Tyr1135} by -56% ($p = 0.0032$). L0+PMA still produced a significant decrease in IGF-1R activation compared to L0 (-55%, $p = 0.0155$). Scramble siRNA in L450 (-57%, $p = 0.0004$) and L0 (-75%, $p < 0.0001$) markedly reduced +IGF-I stimulated IGF-1R β ^{Tyr1135} phosphorylation but had little effect on IGF-1R autophosphorylation compared to L450 and L0 treatment alone. PKC α knockdown in L450 and L0 resulted in -44% ($p = 0.0187$) and -49% ($p = 0.0001$) decreases in IGF-1R^{Tyr1135} phosphorylation, respectively. Compared to scramble, PKC α knockdown in L450 induced a +30% ($p = 0.2347$) increase in IGF-1R activation in L450 and a +99% ($p < 0.0001$) increase in IGF-1R activation in L0.

2.7. PKC α expression is induced by MNR in baboon fetal liver tissue

We next examined the expression of PKC α *in vivo* utilizing the left lobe of baboon fetal liver from a well-established model of MNR associated with moderate FGR (Antonow-Schlorke et al., 2011; Nijland et al., 2010; Cox et al., 2006). PKC α expression was determined by Western blot analysis of control and MNR baboon fetal liver tissue which indicated greater expression of PKC α in MNR (+51%, $p = 0.0326$) at GD 120 (Fig. 12A) and also at GD 165 (+27%, $p = 0.0093$) compared to control (Fig. 12B). These findings were consistent with qualitative IHC data with the same tissue samples. Baboon fetal liver tissue sections also from left lobe showed more prominent immunostaining for PKC α within the parenchyma around the central vein at GD 120 and GD 165 (Fig. 12C-F) both in MNR and control. MNR induced darker staining within the hepatocytes of the parenchyma and around the central vein at GD 120 (Fig. 12D) which remained equally increased at GD 165 (Fig. 12F). These findings demonstrate that PKC α expression is upregulated in MNR at GD 120, preceding the development of FGR which is observable at GD 165. PKC α expression in fetal liver remained elevated at GD 165 (term GD 185). Furthermore, these data are important in suggesting that fetal liver PKC α is sensitive to nutrient restriction *in vivo* due to baboon MNR supporting our *in vitro* data in HepG2 cells showing PKC α activity is nutrient responsive.

3. Discussion

We report compelling evidence that PKC α mediates increased secretion and hyperphosphorylation of IGFBP-1 in response to leucine deprivation. Moreover, we demonstrate that L0 induces PKC α translocation which concomitantly enhances IGFBP-1

expression in a time dependent manner. Our findings that PKC α specifically interacts with IGFBP-1 and CK2 in L0 resulting in IGFBP-1 hyperphosphorylation at sites mediating IGF-I action (Ser101, Ser119 and Ser169) are novel (Abu Shehab et al., 2013). Importantly, our *in vivo* data using fetal liver demonstrate for the first time, greater PKC α expression in baboon fetuses in MNR at GD 120 prior to development of FGR. These findings are consistent with the possibility that nutrient sensitive kinase PKC α mediates increased fetal hepatic IGFBP-1 expression and phosphorylation in FGR.

Perturbation of the IGF-axis by IGFBP-1 has been proposed as an important mechanism linking limited oxygen and nutrient availability to FGR (Martín-Estal et al., 2016; Westwood, 1999). Moreover, IGFBP-1 binding of IGF-I with high affinity is markedly increased by IGFBP-1 phosphorylation at multiple but discrete serine residues (Abu Shehab et al., 2013; Jones et al., 1993b), reducing IGF-I bioavailability which has been associated with FGR (Abu Shehab et al., 2010; Iwashita et al., 1998; Gibson et al., 1999). Although stoichiometric analysis is not available, IGFBP-1 phosphorylation at four discrete sites (pS98, 101, 119 and 169) individually are shown to elicit varied increases in IGF-I affinity and inhibition of IGF-IR activation (Abu Shehab et al., 2013). Importantly the effects on IGF-I action due to phosphorylation at Ser119 were similar to Ser101 (Jones et al., 1993a) and that Ser119 phosphorylation was maximally increased in L0 (Seferovic et al., 2009). IGFBP-1 expression has been shown to be regulated by PKC in HepG2 cells (Lee et al., 1992) however a role for PKC in IGFBP-1 phosphorylation has thus far not been investigated. Studies on PKC in FGR are limited with little implications of the mechanisms involved and are not applicable to FGR or particularly related to IGFBP-1 levels (Langdown et al., 2001; Sugden and Langdown, 2001). More than ten PKC isozymes have been identified in humans Liu and Heckman, (1998) thus, (Sugden and Langdown, 2001) examined placental PKC isoform profiles in the context of placental insufficiency and demonstrated reduced expression of “anti-apoptotic” cPKC isoforms $-\alpha$, $-\beta$ I and $-\beta$ II while induced expression of “pro-apoptotic” nPKC isoforms $-\delta$ and $-\epsilon$. Decreased nutrient availability, believed to be central to the development of FGR, differentially affects the multiple isoforms of PKC with distinct functions in a wide variety of biological systems (Vary et al., 2005; Lee et al., 2008; Lippo BR da et al., 2015; Raveh-Amit et al., 2009; Langdown et al., 2001). Specific fetal liver PKC isoform(s) which regulate fetal growth has not been well established and the mechanisms by which PKC contributes to IGFBP-1 phosphorylation have not been studied, though we have identified the PKC α isoform to be upregulated in baboon FGR and to mediate IGFBP-1 phosphorylation and secretion via its activation in response to leucine deprivation in HepG2 cells. Using PRM-MS and gene silencing, we identified for the first time, the PKC α isoform is associated with IGFBP-1 and mediates its expression and phosphorylation at acidic serine residues in response to leucine deprivation in HepG2 cells. Through conventional inhibitor and activator approaches, we identified respective changes in IGFBP-1 at single sites and close proximity dually phosphorylated IGFBP-1 peptides demonstrating that PKC is positively correlated with IGFBP-1 hyperphosphorylation and that CK2 and PKC act in concert. A previous literature report demonstrated stimulation of CK2 activity by a number of PKC isoforms (Lee et al., 2016). Through multiple approaches (co-IP, PRM-MS, IF and PLA), we provide

convincing data to demonstrate induced interactions between PKC α +CK2 β are consistent with increased IGFBP-1 phosphorylation and expression in response to L0.

Activation of PKC isozymes are associated with its translocation from the cytosol to a membrane compartment (Dempsey et al., 2000; Luria et al., 2000; Hui et al., 2014).). In our study, we used membrane fraction enrichment and IF to demonstrate time dependent PKC α membrane translocation, indicative of PKC α activation in response to L0 which was mimicked by PMA (Hui et al., 2014; Freeley et al., 2011). Concomitantly, IGFBP-1 expression was induced on the same time course as PKC α translocation, linking PKC α activation to increased IGFBP-1 expression in L0. Overall, our findings demonstrate that L0 activates and induces PKC α translocation which is associated with increased IGFBP-1 expression and induces an interaction of PKC α with IGFBP-1 associated with an increase in IGFBP-1 phosphorylation.

Furthermore, we report significant increases in PKC α expression *in vivo* in an established MNR baboon model of FGR at GD 120, preceding the development of FGR which is detectable at GD 165 (Antonow-Schlorke et al., 2011; Nijland et al., 2010; Cox et al., 2006). PKC α expression remained increased at GD 165 (term GD 185). Importantly, fetal liver IGFBP-1 expression and phosphorylation was reported to be increased at the same gestational ages in baboon MNR, suggesting a role for liver PKC in the development of FGR (Abu Shehab et al., 2014; Kakadia et al., 2020).

Furthermore, the IGF-axis is implicated in many different aspects of cellular growth and regulation, including longevity (Junnala et al., 2013; Vitale et al., 2019) and cancer (Weroha and Haluska, 2012). IGFBP-1 has been implicated in regulatory metabolic roles in fat, bone, skeletal tissue and in diabetes (Bach, 2018; Clemmons, 2018) and it is likely that IGFBP-1 phosphorylation may be influencing IGF-I bioavailability in these tissues. Limitations in amino acid availability is a physiological challenge that is relevant for many tissues and organs. It is therefore possible that PKC α regulation of IGFBP-1, which is an inhibitor of cell growth, constitutes a mechanistic link between amino acid deprivation and decreased cell growth in multiple cells and tissues. This work thus can be broadly applicable to many different aspects of cellular growth and regulation, including cancer. Furthermore, our study also demonstrates a mechanistic link between the two highly conserved kinases PKC and CK2 which share commonalities in cell growth and IGF-I signaling in many different diseases (Gould and Newton, 2008; Borgo et al., 2021). We therefore believe that our findings provide significant advance relative to current knowledge broadly in the areas beyond fetal growth restriction.

In summary, PKC α which was identified by PRM-MS, interacts with both IGFBP-1 and CK2 and is associated with increased IGFBP-1 phosphorylation in L0. Furthermore, PKC α gene silencing decreases IGFBP-1 secretion and IGFBP-1 hyperphosphorylation. We report novel mechanisms of nutrient-responsive activation of PKC α in L0 which via its translocation and activation, reduces IGF-I bioavailability through increased IGFBP-1 phosphorylation. Additionally, baboon fetal liver showed greater PKC α expression in FGR. These data provide new insights into the possible role of nutrient-responsive fetal PKC in regulating IGF-I function in the pathophysiology of FGR.

4. Materials and methods

4.1. HepG2 cell culture and L0 treatments

We utilized human hepatocellular carcinoma HepG2 cells as a model for fetal hepatocytes due to their close proteomic and transcriptomic resemblance to fetal hepatocytes in respect to differentiation factors (Kelly and Darlington, 1989; Wilkening et al., 2003; Rowe et al., 2013). The similarities of HepG2 cells to fetal hepatocytes further extends to cultured primary baboon fetal liver cells (Abu Shehab et al., 2014; Li et al., 2013). HepG2 cells at 85% confluency were plated at 5×10^5 and then allowed to adhere for 16 h. Cells were starved for 16 h and subsequently cultured in custom DMEM/F12 media containing either 450 μ M (L450) or 0 μ M (L0) of leucine for 24 h as previously described (Seferovic et al., 2009; Malkani et al., 2015). Conditioned cell media (CM) was collected and cells from L450/L0 were lysed using lysis buffer (Cell Signaling Technologies, Beverly, MA).

4.2. Immunoprecipitation

Immunoprecipitation (IP) of IGFBP-1, CK2 β and PKC was performed using HepG2 cell lysate. For each IP, 100 μ L of 50% Protein A Sepharose slurry (GE Health Care, Canada) was coupled with IGFBP-1 mAb 6303 (Medix Biochemica, Kauniainen, Finland), polyclonal CK2 β (YenZyme, USA) or polyclonal Pan-PKC (SAB4502356, Sigma-Aldrich, USA) respectively. Antibodies were diluted in 5x HEPES buffer (50 mM HEPES, 750 mM NaCl, 15 mM EDTA) and coupled to Protein A Sepharose beads.

HepG2 cell lysate (200 μ g total protein) were buffer exchanged against PBS with 0.1% Tween (PBS-T) using 10K MWCO Ultracel centrifugal filter units (Millipore, Ireland) as described previously (Singal et al., 2018). Unbound proteins were removed (flow-through). For Western blot analysis, proteins from a small aliquot were eluted from Sepharose beads with 50 μ L elution buffer (8 M urea, 5% SDS, 50 mM Tris-HCl pH 7.8) and stored at -20°C . The remaining beads were processed as described below for mass spectrometry.

4.3. SDS-PAGE and Western blotting

Protein separations were conducted using SDS-PAGE with Precision Plus Protein™ All Blue protein standards (BioRad Laboratories, Canada). Proteins were transferred to nitrocellulose membranes, and blocking was performed using either 5% skim milk or 5% bovine serum albumin (BSA) in Tris-buffered saline (TBS) with 0.1% Tween-20 (TBST).

For IGFBP-1 secretion, equal volumes (30–50 μ L) of direct HepG2 CM were obtained using equal number of plated cells used for normalization due to the absence of a secretory internal control. Previously validated (Abu Shehab et al., 2013, 2014) custom phospho-site specific IGFBP-1 antibodies for pSer101 (1:500), pSer119 (1:2000) and pSer169 (1:250) (YenZyme, USA) and a custom polyclonal total IGFBP-1 (1:10,000) (a gift from Dr. Robert Baxter, Australia) were used as primary antibodies. For PKC α , pIGF-1R $\beta^{\text{Tyr}1135}$ and IGF-1R β , equal amounts of total protein in cell lysate from HepG2 cells (30–50 μ g) or from fetal liver extracts were used. Monoclonal PKC α antibody (1:1000) (NB600-201; Novus Biologicals, USA), monoclonal pIGF-1R $\beta^{\text{Tyr}1135}$ (1:1000) (DA7A8; Cell Signalling Technologies, USA), polyclonal IGF-1R β (1:250) (sc-713; Santa-Cruz Biotechnology,

USA) and loading control β -actin (sc-47778; Santa Cruz Biotechnology, USA) were used. Calnexin (1:1000) (610523; BD Biosciences; USA) and α -tubulin (1:20,000) (T5168; Sigma-Aldrich, USA) were used as controls for membrane and cytosol enriched fractions, respectively. Secondary antibodies were HRP-conjugated goat anti-rabbit IgG (1:10,000) and goat anti-mouse IgG (1:10,000) (BioRad, Canada). Precision Protein™ StepTactin-HRP conjugate (BioRad, Canada) was used to visualize the protein ladder and β -actin was used to account for any differences in protein load and transfer. Enhanced chemiluminescence (ECL) reagents were employed for detection of proteins (Mruk and Cheng, 2011). Images were captured using the Quantity One Molecular Imager VersaDoc imaging system (BioRad, Canada) and band intensities were subjected to densitometrical analyses using Image Lab (BioRad, Canada).

4.4. Parallel Reaction Monitoring Mass Spectrometry (PRM-MS)

In-solution digestion of the IP samples was performed as described (Damerill et al., 2016). Peptide digests were desalted using C18-Zip Tip and dried in a Thermo SpeedVac. After desalting and drying, samples were loaded onto a Thermo Easy-Spray analytical column (75 μ m i.d. \times 500 mm) C18 column with an Easy-nLC 1000 chromatography pump. For each analysis, we reconstituted peptides in 20 μ L of 0.1% trifluoroacetic acid (TFA) and loaded 4 μ L onto the column. Peptides were separated on a 125 min (5–40% acetonitrile) gradient. Mass spectra were collected on a Q-Exactive hybrid quadrupole-Orbitrap mass spectrometer coupled to an Easy-nLC 1000 system (ThermoFisher, USA). The spectrometer was set in full MS/data-dependent-MS2 TopN mode: mass analyzer over m/z range of 400–1600 with a mass resolution of 70,000 (at $m/z = 200$), 35 NCE (normalized collision energy), 2.0 m/z isolation window and 15 s dynamic exclusion. The isolation list (not shown) with the Mass [m/z] and the sequences of the peptides used to identify PKC and IGFBP-1 by PRM-MS were recorded. Each trace on the chromatograph represents the detection of each individual transition ion used to monitor PKC detection. Retention time indicates that transition ions result from the same parent peptide (correlating with the time that the parental peptide had eluted from the C18 column). Data were generated by PRM-MS using isolation lists that were specific to PKC and IGFBP-1.

IGFBP-1 internal peptide (NH₂-ALPGEQQPLHALTR-COOH) was used to normalize phosphorylated IGFBP-1. With two possible IGFBP-1 phosphorylation sites (dual), specific transitions were used to distinguish single-site-phosphorylation from each other (specifically, y14, b6 and b9 ions for pSer169 and pSer174; y12 and b15 ions for pSer98 and pS101).

4.5. PKC α siRNA silencing

HepG2 cells were plated at 75% confluence in 6 well plates. Silencing using siRNA against PKC α (SASI_Hs01_00018816; Sigma-Aldrich, USA) in HepG2 cells was achieved using transfection (Abu Shehab et al., 2014) with 80 nM siRNA and 5 μ L Dharmafect transfection reagent (Thermo Scientific, USA) in regular, serum free DMEM:F12 for 24 h. Transfection media was replaced with L450 or L0 media 24 h post transfection. CM and cell lysates were collected from HepG2 cells 48 h post L450 or L0 treatment as described above. Western

immunoblot analysis was used to determine the efficiency of target silencing, total IGFBP-1 secretion and IGFBP-1 phosphorylation at three sites (Ser101, 119 and 169).

4.6. Immunofluorescence (IF)

HepG2 cells were seeded at 2.2×10^5 on 0.1% poly-L-lysine coated coverslips in 6 well plates, followed by L0 treatment. Cells were fixed with 4% paraformaldehyde for 1 h at 4 °C, permeated in 0.25% Triton X-100 for 10 min and blocked with Dako Background Sniper (Biocare Medical, USA) for 10 min.

Several combinations of primary antibodies were used in dual IF: i) mouse mAb PKC α (1:250) and rabbit polyclonal IGFBP-1 (1:2500), ii) mouse mAb PKC α and rabbit polyclonal CK2 β (1:500) and mouse IGFBP-1 mAb 6303 (1:500) and rabbit polyclonal CK2 β (1:500) which were incubated overnight at 4 °C. Single IF staining was performed using mouse mAb PKC α (1:250). Secondary antibodies anti-mouse Alexa Fluor 488 (1:400) and anti-rabbit Alexa Fluor 568 (1:400) were applied to cells and incubated for 45 min. Phalloidin 568 (1:20) was used to stain the cytosol in single IF staining experiments with PKC α (ThermoFisher, Canada). Cells were then counterstained with DAPI (1:300) (Life Technologies, Canada). Negative controls used were rabbit (X0903) and mouse pre-immune serum (X0931) at 4 μ g/mL (Agilent Technologies, Santa Clara, CA). Coverslips were mounted (Fisher Scientific, Fairlawn, NJ) with Prolong Gold Mounting Media (ThermoFisher, Canada) and dried overnight prior to imaging on an Nikon Inverted T12E Deconvolution Microscope (Nikon Instruments Inc. USA).

4.7. Proximity ligation assay (PLA)

HepG2 cells were seeded at 2.2×10^5 on 0.1% poly-L-lysine coated coverslips in 6 well plates, followed by L0 treatment as described earlier. Cells were fixed and permeabilized as in IF. Primary antibody combinations and incubation time remained the same as in dual IF.

Fixed HepG2 cells blocked with Duolink blocking solution (Sigma Aldrich, USA) were used for PLA using PLA secondary probes (antirabbit plus and anti-mouse minus) diluted 1:5 in Duolink antibody diluent (Sigma-Aldrich, USA) and incubated for 1 h at room temperature. Subsequent ligation and amplification were performed according to manufacturer's instructions (Sigma-Aldrich, USA). Samples were mounted with provided mounting media containing DAPI counterstain and image acquisition was acquired on an AxioImager Z1 Epifluorescent Microscope (Carl Zeiss Canada Ltd.). Quantification was performed through automated counting of PLA signals and cell nuclei using ImagePro Premier and normalized by the cell number. Data were analyzed in GraphPad Prism 6.

4.8. Treatment of HepG2 cells by pharmacological kinase inhibitors and activators

HepG2 cells were plated at 75% confluence and starved for 16 h in 0% FBS (DMEM:F12) prior to treatments with inhibitors and/or activators. Following dose dependency treatments, subsequent experiments utilized PKC activator phorbol 12-myristate 13-acetate (PMA) at 100 nM; PKC inhibitor bisindolylmaleimide II (Bis II) at 7.5 μ M and CK2 inhibitor 4,5,6,7-tetrabromobenzotriazole (TBB) at 10 μ M (Malkani et al., 2016). Following 24 h of pharmacological treatment, CM and cell lysate were collected using lysis buffer (Cell

Signaling Technologies, Beverly, MA) with protease and phosphatase inhibitor cocktails (P8340, P5726, P0044; Sigma-Aldrich, St. Louis, MO). Protein contents determined by Bradford assay (BioRad Laboratories, Canada) and samples were stored at -20°C .

4.9. Subcellular fractionation of HepG2 cells by differential centrifugation

HepG2 cells at 80% confluency were detached with 10 mM EDTA in PBS for 35 min. Cells were collected and centrifuged at 400 g for 4 min and resuspended 1:5 in homogenization buffer (0.25 M sucrose, 5 mM HEPES, pH 7.4, cold) with protease and phosphatase inhibitors (same as used for cell lysis). Cells were homogenized utilizing a Polytron PT3000 (Kinematica AG, Lucerne, Switzerland). Post-nuclear cell lysate was obtained by nuclear extraction by centrifugation at 2000 g for 10 min. Post-nuclear cell lysate was centrifuged at $105,000\times g$ for 1 h and the supernatant (cytosolic fraction) was collected, the pellet (membrane fraction) rinsed with homogenization buffer and then resuspended in homogenization buffer containing 0.1% Triton X-100. The supernatant and pellet fractions were then sonicated and stored at -20°C for analysis by Western blot.

4.10. Confocal image acquisition

Images were captured with a $63\times$ Plan-Apochromat oil immersion lens on a Leica SP8 confocal microscope. The acousto-optical beamsplitters were tuned to avoid all crosstalk between channels. Alexa 488 was excited with a blue 20 mW 488 nm HeNe laser. For Alexa 568, a green 20 mW 552 nm HeNe laser was used for excitation. DAPI signal was excited with a 50 mW 405–50 Diode.

4.11. IGF-1R autophosphorylation assay

We employed our IGF-1R autophosphorylation assay as previously described (Abu Shehab et al., 2013). In brief, mouse embryo fibroblast P6 cells (a BALB/c3T3 cells derivative) which over-express human IGF-1R (a kind gift from Dr. R Baserga, Thomas Jefferson University, Philadelphia, PA) were seeded at 4×10^5 in 6-well plates and allowed to adhere overnight. P6 cells were starved for 6 h, then treated with HepG2 cell conditioned media from several treatments containing equal amounts of total IGFBP-1 incubated for 2 h with rhIGF-I (25 ng/mL) for 15 min at room temperature. P6 cells were lysed and equal amount of total protein (40 μg) was loaded for Western blotting to assess changes in IGF-1R autophosphorylation using pIGF-1R $\beta^{\text{Tyr}1135}$ antibody.

4.12. Cell viability assay

Standard Trypan Blue exclusion assay was utilized to ensure that pharmacological or siRNA treatments did not negatively impact cell viability. Following treatments, cells were lifted and re-suspended in 10% FBS media and diluted 1:1 with 0.4% trypan blue and counted manually with a haemocytometer.

4.13. Preparation of baboon fetal liver extracts

Baboon fetal liver tissue were obtained at GD 120 and 165 (full term 185 days). Frozen pieces (-80°C) of the left lobe (~ 0.2 g) of fetal liver (GD 120; n = 19; male = 11; female = 8, GD 165; n = 24, male = 10; female = 14) were homogenized using lysis buffer with protease

and phosphatase inhibitor cocktails described in detail previously (Kakadia et al., 2020). The homogenate was centrifuged, and the clear supernatant was stored at -80°C .

4.14. Immunohistochemistry (IHC) using baboon fetal liver tissue

Tissues sections ($5\ \mu\text{m}$) from GD matched control and MNR liver tissue of the left lobe were mounted on the same microscope slides and baked overnight at 45°C . Slides were deparaffinized in Xylene, rehydrated through graded ethanol series, then washed in tap water followed by PBS. Endogenous peroxidases were blocked in 3% hydrogen peroxide, and tissues were incubated with Background Sniper blocking solution (Biocare Medical, LLC., Pacheco, CA). Slides were incubated overnight at 4°C with mouse PKC α mAb (1:250) (Novus Biologicals, USA) in antibody diluent (Dako, Agilent Technologies, Santa Clara, CA). Secondary antibodies (anti-mouse horseradish peroxidase polymer complex, ImmPRESS $^{\text{®}}$ HRP Reagent Kit, Vector Laboratories, Burlingame, CA) were incubated for 45 min at room temperature. Sections were treated with 3,3'-diaminobenzidine (DAB) substrate (ImmPACT $^{\text{®}}$ DAB Peroxidase Substrate Kit, Vector Laboratories, Burlingame, CA) for 2 min, counter-stained with Modified Mayer's Hematoxylin (ThermoFisher, USA) for 20 s, rinsed, immersed in tap water for 4 min, then dehydrated through graded alcohols, cleared with Xylene, and mounted with Permount (Fisher Scientific, Inc.) for 30 s. Images were captured with a Zeiss AxioImager Z1 Microscope (Carl Zeiss Canada Ltd., North York, ON Canada) using brightfield imaging with a 40x oil immersion lens.

4.15. Data presentation and statistics

Data was analyzed using GraphPad Prism 6 (GraphPad Software, USA). Quantification of controls were assigned an arbitrary value of 1 and treatments were expressed relative to this mean. All quantified experiments were performed at minimum in triplicate. Statistical significance was tested using paired *t*-test, one-way analysis of variance (ANOVA) or two-way ANOVA with Dunnett's Multiple Comparison Post-Test and expressed as the mean + SEM. Significance was accepted at $p < 0.05$.

Supplementary Material

Refer to Web version on PubMed Central for supplementary material.

Acknowledgements

We thank Dr. Robert Baxter (Kolling Institute of Medical Research, University of Sydney, Sydney, Australia) for his kind gift of IGFBP-1 polyclonal antibody; and Biotron Integrated Microscopy, University of Western Ontario, in aiding immunohistochemistry, dual immunofluorescent and PLA image acquisition, quantification automation and analyses.

Funding

This work was supported by grants from the Natural Sciences and Engineering Research Council of Canada (NSERC), Discovery Grant (RGPN to MBG), the National Institute of Health (R03HD078313 to MBG and TJ), Program Project grant (P01HD021350 and R03HD093950 to PWN). AC received Children's Health Research Institute and Department of Pediatrics Graduate Studentship Awards (University of Western Ontario).

References

- Abu Shehab M, Khosravi J, Han VKM, Shilton BH, Gupta MB, 2010 4 5. Site-specific IGFBP-1 hyper-phosphorylation in fetal growth restriction: clinical and functional relevance. *J. Proteome Res* 9 (4), 1873–1881. [PubMed: 20143870]
- Abu Shehab M, Iosef C, Wildgruber R, Sardana G, Gupta MB, 2013 3. Phosphorylation of IGFBP-1 at discrete sites elicits variable effects on IGF-I receptor autophosphorylation. *Endocrinology* 154 (3), 1130–1143. [PubMed: 23354097]
- Abu Shehab M, Damerill I, Shen T, Rosario FJ, Nijland M, Nathanielsz PW, et al. , 2014 4. Liver mTOR controls IGF-I bioavailability by regulation of protein kinase CK2 and IGFBP-1 phosphorylation in fetal growth restriction. *Endocrinology* 155 (4), 1327–1339. [PubMed: 24437487]
- Ankrapp DP, Jones JI, Clemmons DR, 1996 3 1. Characterization of insulin-like growth factor binding protein-1 kinases from human hepatoma cells. *J. Cell. Biochem* 60 (3), 387–399. [PubMed: 8867814]
- Antonow-Schlorke I, Schwab M, Cox LA, Li C, Stuchlik K, Witte OW, et al. , 2011 2 15. Vulnerability of the fetal primate brain to moderate reduction in maternal global nutrient availability. *Proc. Natl. Acad. Sci. U. S. A* 108 (7), 3011–3016. [PubMed: 21252306]
- Bach LA, 2018 7 1. IGF-binding proteins. *J. Mol. Endocrinol* 61 (1), T11–T28. [PubMed: 29255001]
- Borgo C, D'Amore C, Sarno S, Salvi M, Ruzzene M, 2021 5 17. Protein kinase CK2: a potential therapeutic target for diverse human diseases. *Signal Transduct Target Ther* 6 (1), 1–20. [PubMed: 33384407]
- Cetin I, Marconi AM, Bozzetti P, Sereni LP, Corbetta C, Pardi G, et al. , 1988 1. Umbilical amino acid concentrations in appropriate and small for gestational age infants: a biochemical difference present in utero. *Am. J. Obstet. Gynecol* 158 (1), 120–126. [PubMed: 3337158]
- Cetin I, Corbetta C, Sereni LP, Marconi AM, Bozzetti P, Pardi G, et al. , 1990 1. Umbilical amino acid concentrations in normal and growth-retarded fetuses sampled in utero by cordocentesis. *Am. J. Obstet. Gynecol* 162 (1), 253–261. [PubMed: 2301500]
- Chard T, 1994 9. Insulin-like growth factors and their binding proteins in normal and abnormal human fetal growth. *Growth Regul.* 4 (3), 91–100. [PubMed: 7532055]
- Clemmons DR, 2018 7 1. Role of IGF-binding proteins in regulating IGF responses to changes in metabolism. *J. Mol. Endocrinol* 61 (1), T139–T169. [PubMed: 29563157]
- Coverley JA, Baxter RC, 1997 4 4. Phosphorylation of insulin-like growth factor binding proteins. *Mol. Cell. Endocrinol* 128 (1–2), 1–5. [PubMed: 9140069]
- Cox LA, Nijland MJ, Gilbert JS, Schlabritz-Loutsevitch NE, Hubbard GB, McDonald TJ, et al. , 2006 4 1. Effect of 30 per cent maternal nutrient restriction from 0.16 to 0.5 gestation on fetal baboon kidney gene expression. *J Physiol* 572 (Pt 1), 67–85. [PubMed: 16513668]
- Damerill I, Biggar KK, Abu Shehab M, Li SS-C, Jansson T, Gupta MB, 2016 2. Hypoxia increases IGFBP-1 phosphorylation mediated by mTOR inhibition. *Mol. Endocrinol* 30 (2), 201–216. [PubMed: 26714229]
- Dempsey EC, Newton AC, Mochly-Rosen D, Fields AP, Reyland ME, Insel PA, et al. , 2000 9. Protein kinase C isozymes and the regulation of diverse cell responses. *Am. J. Physiol. Lung Cell Mol. Physiol* 279 (3), L429–L438. [PubMed: 10956616]
- Freeley M, Kelleher D, Long A, 2011 5. Regulation of Protein Kinase C function by phosphorylation on conserved and non-conserved sites. *Cell. Signal* 23 (5), 753–762. [PubMed: 20946954]
- Gibson JM, Westwood M, Lauszus FF, Klebe JG, Flyvbjerg A, White A, 1999 2. Phosphorylated insulin-like growth factor binding protein 1 is increased in pregnant diabetic subjects. *Diabetes* 48 (2), 321–326. [PubMed: 10334308]
- Gibson JM, Aplin JD, White A, Westwood M, 2001 1. Regulation of IGF bioavailability in pregnancy. *Mol. Hum. Reprod* 7 (1), 79–87. [PubMed: 11134364]
- Girmita L, Worrall C, Takahashi S-I, Seregard S, Girmita A, 2014 7. Something old, something new and something borrowed: emerging paradigm of insulin-like growth factor type 1 receptor (IGF-1R) signaling regulation. *Cell Mol Life Sci CMLS* 71 (13), 2403–2427. [PubMed: 24276851]

- Gong Y, Ballejo G, Alkhalaf B, Molnar P, Murphy LC, Murphy LJ, 1992 12. Phorbol esters differentially regulate the expression of insulin-like growth factor binding proteins in endometrial carcinoma cells. *Endocrinology* 131 (6), 2747–2754. [PubMed: 1280205]
- Gould CM, Newton AC, 2008 8. The life and death of protein kinase C. *Curr. Drug Targets* 9 (8), 614–625. [PubMed: 18691009]
- Han VK, Matsell DG, Delhanty PJ, Hill DJ, Shimasaki S, Nygard K, 1996. IGF-binding protein mRNAs in the human fetus: tissue and cellular distribution of developmental expression. *Horm. Res* 45 (3–5), 160–166. [PubMed: 8964576]
- Hui X, Kaestner L, Lipp P, 2014 12 1. Differential targeting of cPKC and nPKC decodes and regulates Ca²⁺ and lipid signalling. *Biochem. Soc. Trans* 42 (6), 1538–1542. [PubMed: 25399567]
- Iwashita M, Sakai K, Kudo Y, Takeda Y, 1998 12. Phosphoisoforms of insulin-like growth factor binding protein-1 in appropriate-for-gestational-age and small-for-gestational-age fetuses. *Growth Horm IGF Res Off J Growth Horm Res Soc Int IGF Res Soc* 8 (6), 487–493.
- Jones JI, Busby WH, Wright G, Smith CE, Kimack NM, Clemmons DR, 1993 1 15. Identification of the sites of phosphorylation in insulin-like growth factor binding protein-1. Regulation of its affinity by phosphorylation of serine 101. *J. Biol. Chem* 268 (2), 1125–1131. [PubMed: 7678248]
- Jones JI, Busby WH, Wright G, Clemmons DR, 1993 3. Human IGFBP-1 is phosphorylated on 3 serine residues: effects of site-directed mutagenesis of the major phosphoserine. *Growth Regul.* 3 (1), 37–40. [PubMed: 7683525]
- Jousse C, Bruhat A, Ferrara M, Fafournoux P, 1998 8 15. Physiological concentration of amino acids regulates insulin-like-growth-factor-binding protein 1 expression. *Biochem. J* 334 (Pt 1), 147–153. [PubMed: 9693114]
- Junnila RK, List EO, Berryman DE, Murrey JW, Kopchick JJ, 2013 6. The GH/IGF-1 axis in ageing and longevity. *Nat. Rev. Endocrinol* 9 (6), 366–376. [PubMed: 23591370]
- Kakadia JH, Jain BB, Biggar K, Sutherland A, Nygard K, Li C, et al. , 2020 01. Hyperphosphorylation of fetal liver IGFBP-1 precedes slowing of fetal growth in nutrient-restricted baboons and may be a mechanism underlying IUGR. *Am. J. Physiol. Endocrinol. Metab* 319 (3), E614–E628. [PubMed: 32744097]
- Kelly JH, Darlington GJ, 1989 2. Modulation of the liver specific phenotype in the human hepatoblastoma line Hep G2. *Vitro Cell Dev Biol J Tissue Cult Assoc* 25 (2), 217–222.
- Koistinen R, Angervo M, Leinonen P, Hakala T, Seppälä M, 1993 6 16. Phosphorylation of insulin-like growth factor-binding protein-1 increases in human amniotic fluid and decidua from early to late pregnancy. *Clin Chim Acta Int J Clin Chem* 215 (2), 189–199.
- Langdown ML, Holness MJ, Sugden MC, 2001 4. Early growth retardation induced by excessive exposure to glucocorticoids in utero selectively increases cardiac GLUT1 protein expression and Akt/protein kinase B activity in adulthood. *J. Endocrinol* 169 (1), 11–22. [PubMed: 11250642]
- Lee PD, Abdel-Maguid LS, Snuggs MB, 1992 8. Role of protein kinase-C in regulation of insulin-like growth factor-binding protein-1 production by HepG2 cells. *J. Clin. Endocrinol. Metab* 75 (2), 459–464. [PubMed: 1379255]
- Lee MY, Jo SD, Lee JH, Han HJ, 2008 12 15. L-leucine increases [3H]-thymidine incorporation in chicken hepatocytes: involvement of the PKC, PI3K/Akt, ERK1/2, and mTOR signaling pathways. *J. Cell. Biochem* 105 (6), 1410–1419. [PubMed: 18980246]
- Lee Y-H, Park J-W, Bae Y-S, 2016 2. Regulation of protein kinase CK2 catalytic activity by protein kinase C and phospholipase D2. *Biochimie* 121, 131–139. [PubMed: 26703243]
- Li C, Shu Z-J, Lee S, Gupta MB, Jansson T, Nathanielsz PW, et al. , 2013 8. Effects of maternal nutrient restriction, IUGR, and glucocorticoid exposure on phosphoenolpyruvate carboxykinase-1 expression in fetal baboon hepatocytes in vitro. *J. Med. Primatol* 42 (4), 211–219. [PubMed: 23600855]
- Lippo Br da S, Batista TM, de Rezende LF, Cappelli AP, Camargo RL, Branco RCS, et al. , 2015 5. Low-protein diet disrupts the crosstalk between the PKA and PKC signaling pathways in isolated pancreatic islets. *J. Nutr. Biochem* 26 (5), 556–562. [PubMed: 25736482]
- Litchfield DW, 2003 1 1. Protein kinase CK2: structure, regulation and role in cellular decisions of life and death. *Biochem. J* 369 (Pt 1), 1–15. [PubMed: 12396231]

- Liu WS, Heckman CA, 1998 9. The sevenfold way of PKC regulation. *Cell. Signal* 10 (8), 529–542. [PubMed: 9794251]
- Liu JP, Baker J, Perkins AS, Robertson EJ, Efstratiadis A, 1993 10 8. Mice carrying null mutations of the genes encoding insulin-like growth factor I (Igf-1) and type 1 IGF receptor (Igf1r). *Cell* 75 (1), 59–72. [PubMed: 8402901]
- Luria A, Tennenbaum T, Sun QY, Rubinstein S, Breitbart H, 2000 6. Differential localization of conventional protein kinase C isoforms during mouse oocyte development. *Biol. Reprod* 62 (6), 1564–1570. [PubMed: 10819756]
- Malkani N, Jansson T, Gupta MB, 2015 9 5. IGFBP-1 hyperphosphorylation in response to leucine deprivation is mediated by the AAR pathway. *Mol. Cell. Endocrinol* 412, 182–195. [PubMed: 25957086]
- Malkani N, Biggar K, Shehab MA, Li S, Jansson T, Gupta MB, 2016 4 15. Increased IGFBP-1 phosphorylation in response to leucine deprivation is mediated by CK2 and PKC. *Mol. Cell. Endocrinol* 425, 48–60. [PubMed: 26733150]
- Martín-Estal I, de la Garza RG, Castilla-Cortázar I, 2016. Intrauterine growth retardation (IUGR) as a novel condition of insulin-like growth factor-1 (IGF-1) deficiency. *Rev. Physiol. Biochem. Pharmacol* 170, 1–35. [PubMed: 26634242]
- Matsukawa T, Inoue Y, Oishi Y, Kato H, Noguchi T, 2001 11. Up-regulation of upstream stimulatory factors by protein malnutrition and its possible role in regulation of the IGF-binding protein-1 gene. *Endocrinology* 142 (11), 4643–4651. [PubMed: 11606429]
- Meggio F, Pinna LA, 2003 3. One-thousand-and-one substrates of protein kinase CK2? *FASEB J Off Publ Fed Am Soc Exp Biol* 17 (3), 349–368.
- Mruk DD, Cheng CY, 2011. Enhanced chemiluminescence (ECL) for routine immunoblotting. *Spermatogenesis* 1 (2), 121–122. [PubMed: 22319660]
- Murphy VE, Smith R, Giles WB, Clifton VL, 2006 4. Endocrine regulation of human fetal growth: the role of the mother, placenta, and fetus. *Endocr. Rev* 27 (2), 141–169. [PubMed: 16434511]
- Ng T, Squire A, Hansra G, Bormancin F, Prevostel C, Hanby A, et al. , 1999 3 26. Imaging protein kinase Calpha activation in cells. *Science* 283 (5410), 2085–2089. [PubMed: 10092232]
- Nijland MJ, Mitsuya K, Li C, Ford S, McDonald TJ, Nathanielsz PW, et al. , 2010 4 15. Epigenetic modification of fetal baboon hepatic phosphoenolpyruvate carboxykinase following exposure to moderately reduced nutrient availability. *J Physiol* 588 (Pt 8), 1349–1359. [PubMed: 20176628]
- Popovici RM, Lu M, Bhatia S, Faessen GH, Giaccia AJ, Giudice LC, 2001 6. Hypoxia regulates insulin-like growth factor-binding protein 1 in human fetal hepatocytes in primary culture: suggestive molecular mechanisms for in utero fetal growth restriction caused by uteroplacental insufficiency. *J. Clin. Endocrinol. Metab* 86 (6), 2653–2659. [PubMed: 11397868]
- Raveh-Amit H, Maissel A, Poller J, Marom L, Elroy-Stein O, Shapira M, et al. , 2009 11. Translational control of protein kinase c η by two upstream open reading frames. *Mol. Cell Biol* 29 (22), 6140–6148. [PubMed: 19797084]
- Rowe C, Gerrard DT, Jenkins R, Berry A, Durkin K, Sundstrom L, et al. , 2013 8. Proteome-wide analyses of human hepatocytes during differentiation and dedifferentiation. *Hepatology* 58 (2), 799–809.
- Seferovic MD, Ali R, Kamei H, Liu S, Khosravi JM, Nazarian S, et al. , 2009 1. Hypoxia and leucine deprivation induce human insulin-like growth factor binding protein-1 hyperphosphorylation and increase its biological activity. *Endocrinology* 150 (1), 220–231. [PubMed: 18772238]
- Singal SS, Nygard K, Dhruv MR, Biggar K, Shehab MA, Li SS-C, et al. , 2018. Co-localization of insulin-like growth factor binding protein-1, casein kinase-2 β , and mechanistic target of rapamycin in human hepatocellular carcinoma cells as demonstrated by dual immunofluorescence and in situ proximity ligation assay. *Am. J. Pathol* 188 (1), 111–124. [PubMed: 29037858]
- Steinberg SF, 2008 10. Structural basis of protein kinase C isoform function. *Physiol. Rev* 88 (4), 1341–1378. [PubMed: 18923184]
- Straus DS, Burke EJ, Marten NW, 1993 3. Induction of insulin-like growth factor binding protein-1 gene expression in liver of protein-restricted rats and in rat hepatoma cells limited for a single amino acid. *Endocrinology* 132 (3), 1090–1100. [PubMed: 7679969]

- Sugden MC, Langdown ML, 2001 12 20. Possible involvement of PKC isoforms in signalling placental apoptosis in intrauterine growth retardation. *Mol. Cell. Endocrinol* 185 (1–2), 119–126. [PubMed: 11738801]
- Tazuke SI, Mazure NM, Sugawara J, Carland G, Faessen GH, Suen L-F, et al. , 1998 8 18. Hypoxia stimulates insulin-like growth factor binding protein 1 (IGFBP-1) gene expression in HepG2 cells: a possible model for IGFBP-1 expression in fetal hypoxia. *Proc. Natl. Acad. Sci. U. S. A* 95 (17), 10188–10193. [PubMed: 9707622]
- Vary TC, Goodman S, Kilpatrick LE, Lynch CJ, 2005 10. Nutrient regulation of PKCepsilon is mediated by leucine, not insulin, in skeletal muscle. *Am. J. Physiol. Endocrinol. Metab* 289 (4), E684–E694. [PubMed: 15886222]
- Vitale G, Pellegrino G, Vollery M, Hofland LJ, 2019. ROLE of IGF-1 system in the modulation of longevity: controversies and new insights from a centenarians' perspective. *Front. Endocrinol* 10 (27) 10.3389/fendo.2019.00027. Published 2019 2 1.
- Webb BLJ, Hirst SJ, Giembycz MA, 2000 8. Protein kinase C isoenzymes: a review of their structure, regulation and role in regulating airways smooth muscle tone and mitogenesis. *Br. J. Pharmacol* 130 (7), 1433–1452. [PubMed: 10928943]
- Weroha SJ, Haluska P, 2012 6. IGF system in cancer. *Endocrinol Metab. Clin. N. Am* 41 (2), 335–350.
- Westwood M, 1999 9. Role of insulin-like growth factor binding protein 1 in human pregnancy. *Rev. Reprod* 4 (3), 160–167. [PubMed: 10521153]
- Wilkening S, Stahl F, Bader A, 2003 8. Comparison of primary human hepatocytes and hepatoma cell line Hepg2 with regard to their biotransformation properties. *Drug Metab Dispos Biol Fate Chem* 31 (8), 1035–1042. [PubMed: 12867492]
- Yu J, Iwashita M, Kudo Y, Takeda Y, 1998 2. Phosphorylated insulin-like growth factor (IGF)-binding protein-1 (IGFBP-1) inhibits while non-phosphorylated IGFBP-1 stimulates IGF-I-induced amino acid uptake by cultured trophoblast cells. *Growth Horm IGF Res Off J Growth Horm Res Soc Int IGF Res Soc* 8 (1), 65–70.

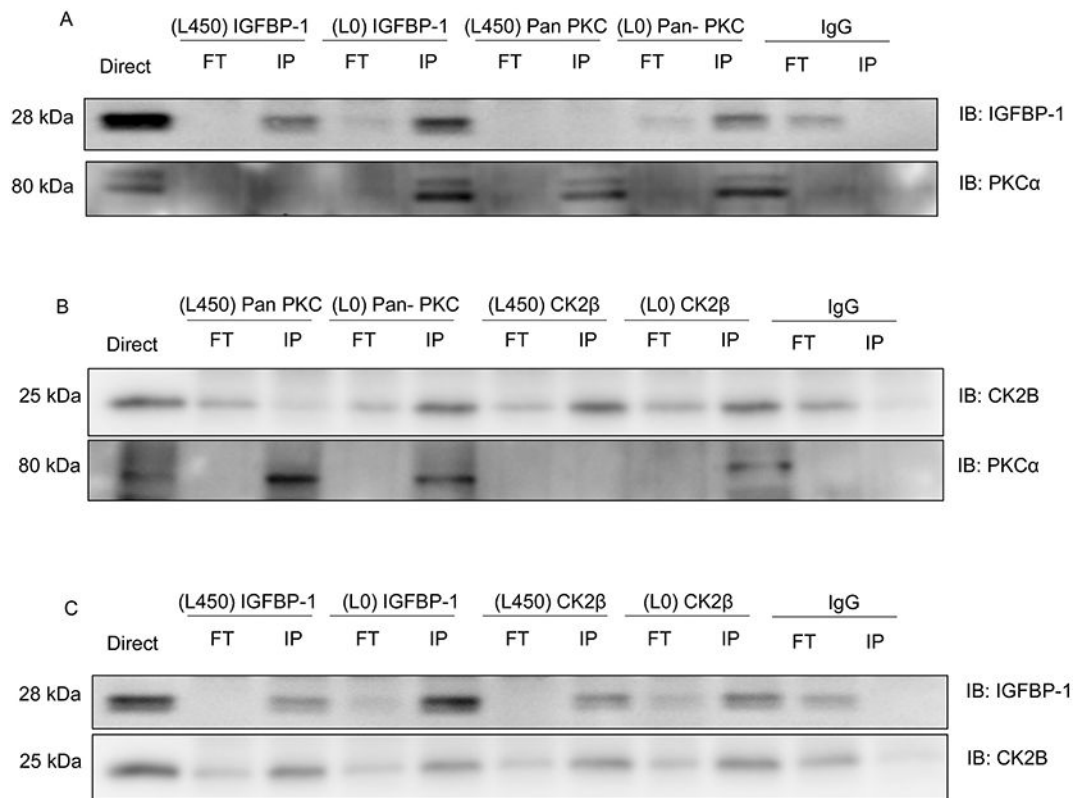


Fig. 1. IGFBP-1, CK2 β and PKC α reciprocally co-immunoprecipitated in L0 conditions. HepG2 cells were cultured in L450 and L0 media, lysed and immunoprecipitated (IP) using total IGFBP-1 (mAb 6303), polyclonal CK2 β , polyclonal pan-PKC antibodies and rabbit pre-immune serum (IgG). **(A)** IP of IGFBP-1 and PKC α demonstrating reciprocal IGFBP-1+PKC α co-IP in L0. **(B)** IP of PKC α and CK2 β demonstrating reciprocal PKC α +CK2 β co-IP in L0. **(C)** IP of IGFBP-1 and CK2 β demonstrating reciprocal IGFBP-1+CK2 β co-IP in L450 and L0. The IP'd proteins were immunoblotted for total IGFBP-1 using polyclonal IGFBP-1, polyclonal CK2 β , and mAb PKC α antibodies. Immunoprecipitation using rabbit IgG failed to IP IGFBP-1, PKC α and CK2 β .

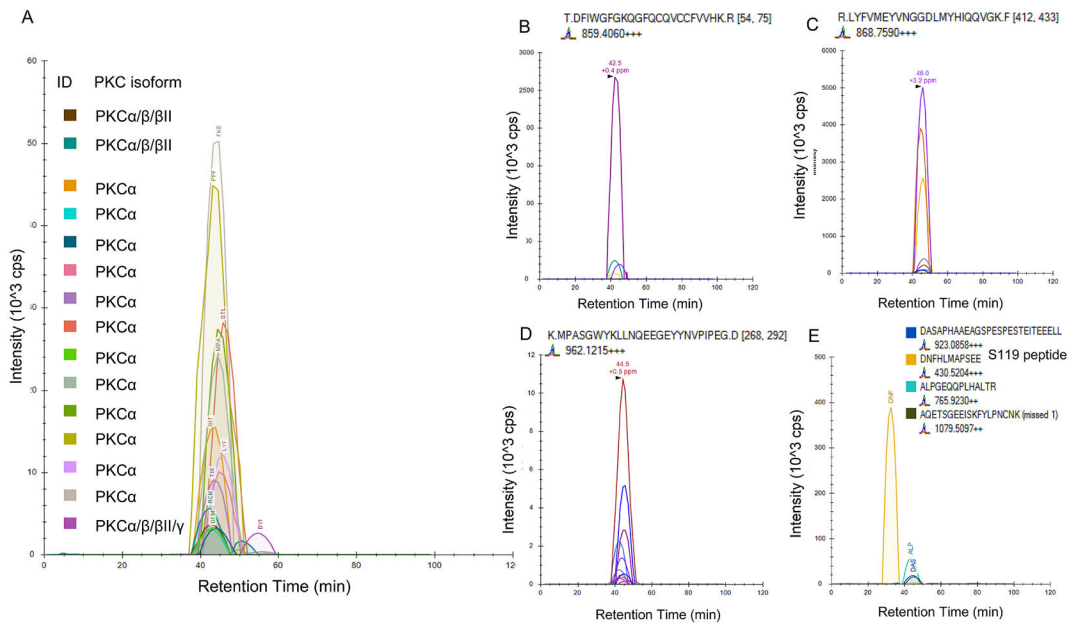


Fig. 2. PKC interaction with IGFBP-1 and CK2β in L0.

HepG2 cells cultured in L0 media were independently IP'd using anti-IGFBP-1 and anti-CK2β antibodies and analyzed by PRM-MS. **(A)** Detection of PKC peptides by PRM-MS from IGFBP-1 immunoprecipitation. Chromatogram shows total transitions for 15 PKC-specific peptides, each peak monitor at least 4 daughter ions. **(B–D)** Representative spectra of each daughter ion used to detect the presence of PKC from IP samples. **(E)** Codetection of IGFBP-1 protein. Chromatogram shows total transitions for 4 IGFBP-1 peptides, each peak monitors at least four daughter ions. All samples were doubly digested by trypsin and Asp-N protease and C18 cleaned prior to MS.

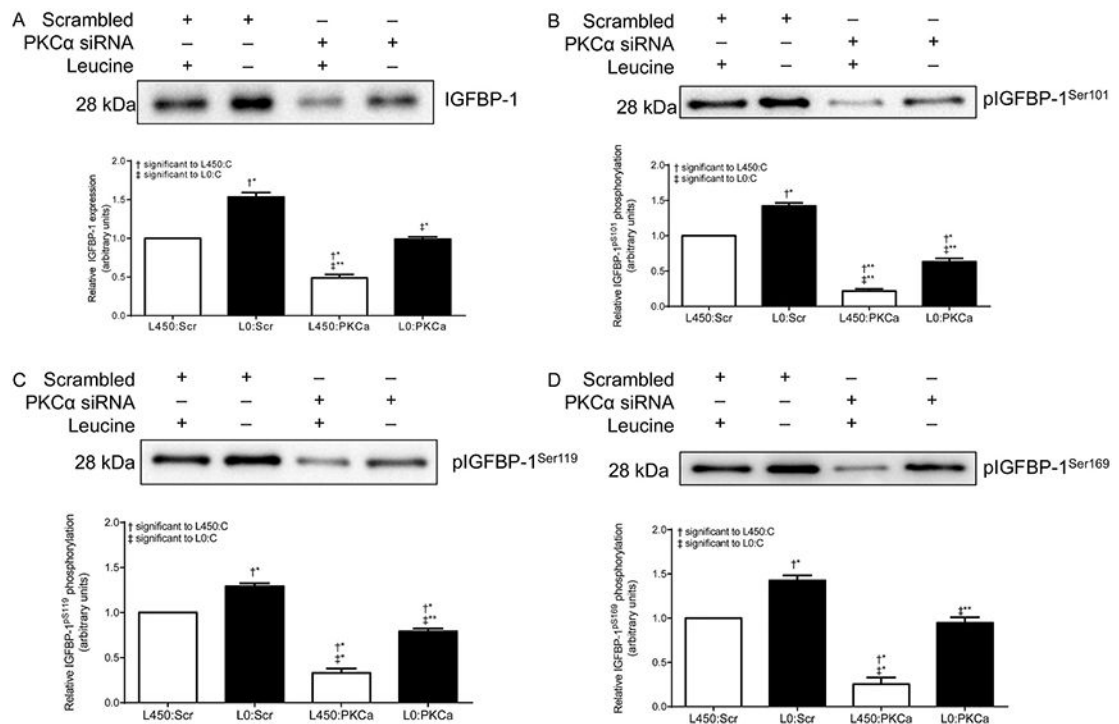


Fig. 3. The effect of PKC α silencing on IGFBP-1 secretion and phosphorylation.

HepG2 cells were treated with scrambled or PKC α siRNA for 24 h and subsequently cultured in L450 or L0 media for 48 h ($n = 3$ each). Representative western blots of conditioned HepG2 CM indicating (A) total IGFBP-1 and IGFBP-1 phosphorylation at (B) Ser101, (C) Ser119 and (D) Ser169. Values are displayed as mean + SEM. * $p < 0.05$, ** $p = 0.001-0.05$, *** $p < 0.0001$ versus control; One-way analysis of variance; Dunnet's Multiple Comparison Test; $n = 3$.

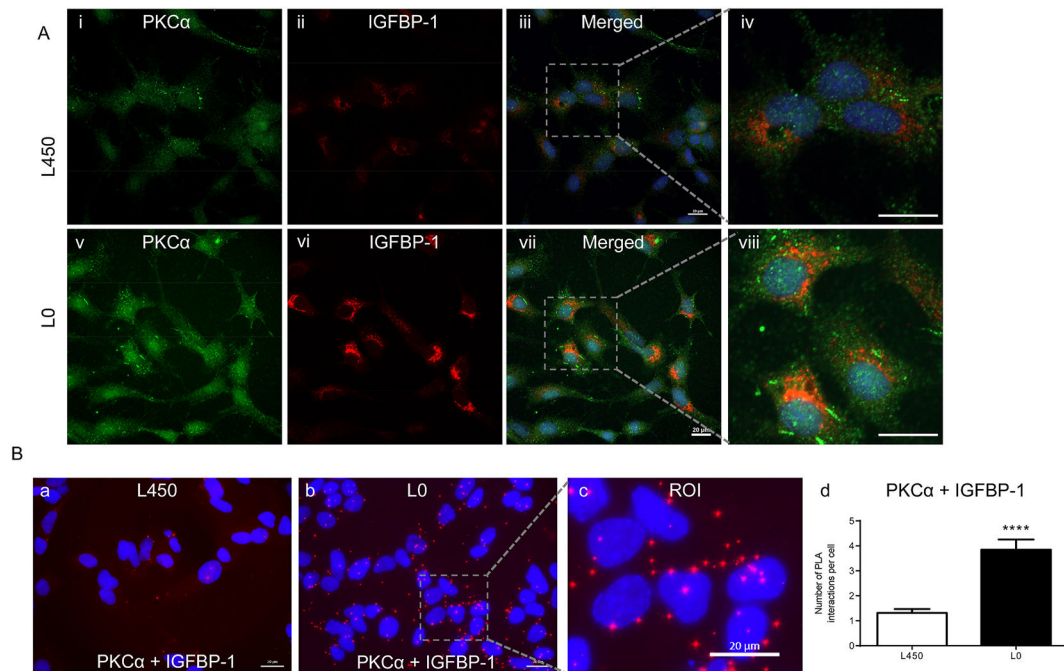


Fig. 4. L0 mediates PKC α interaction with IGFBP-1.

HepG2 cells were cultured in L450 or L0 media and (A) immunostained to visualize (i, v) PKC α (green) with (ii, vi) IGFBP-1 (red). (iii, vii) Merged images demonstrate co-localization of PKC α and IGFBP-1. (iv, viii) Region of interest within merged channel images. (B) Proximity ligation assay (PLA) for PKC α and IGFBP-1 in (a) L450 and (b) L0 conditions. (c) Region of interest of proximity interactions between PKC α and IGFBP-1 in L0 conditions. (d) Number of PLA signals (red dots) per cell for PKC α and IGFBP-1 proximity reactions in HepG2 cells cultured in L450 and L0 media. Values are displayed as mean + SEM. * $p < 0.05$, ** $p = 0.001-0.05$, *** $p < 0.0001$ versus control; paired t -test; Dunnet's Multiple Comparison Test; $n = 3$. Scale bars: 20 μm .

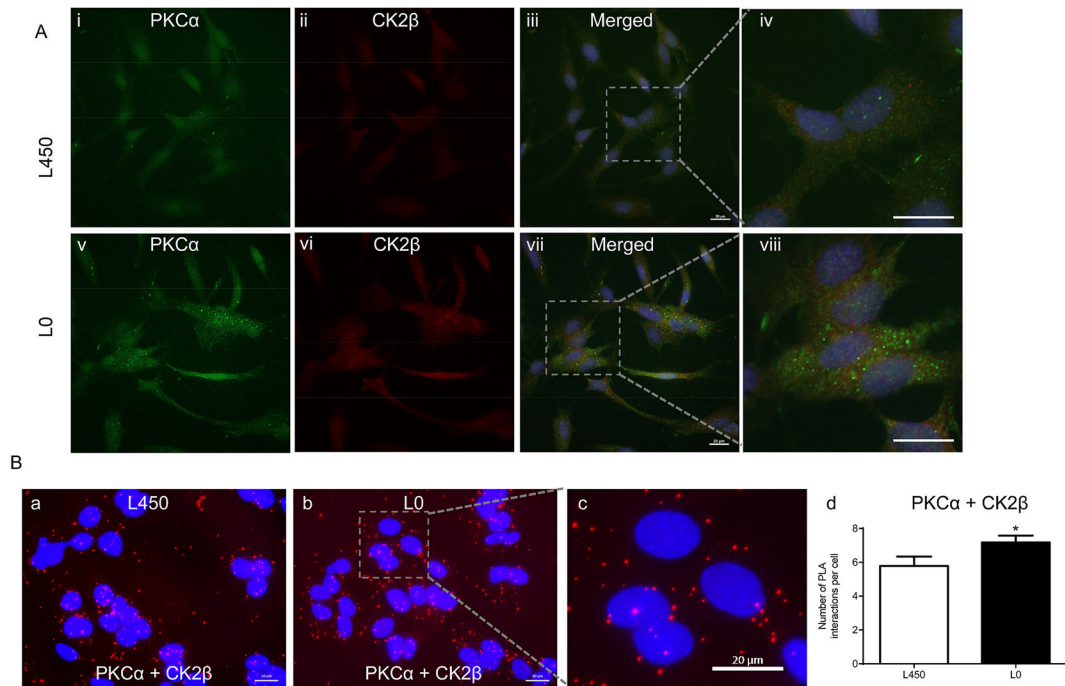


Fig. 5. L0 mediates PKC α interaction with CK2 β .

HepG2 cells were cultured in L450 or L0 media and (A) immunostained to visualize (i, v) PKC α (green) with (ii, vi) CK2 β (red). (iii, vii) Merged images demonstrate co-localization of PKC α and CK2 β . (iv, viii) Region of interest within merged channel images. (B) Proximity ligation assay (PLA) for PKC α and CK2 β in (a) L450 and (b) L0 conditions. (c) Region of interest of proximity interactions between PKC α and CK2 β in L0 conditions. (d) Number of PLA signals (red dots) per cell for PKC α and CK2 β proximity reactions in HepG2 cells cultured in L450 and L0 media. Values are displayed as mean + SEM. * $p < 0.05$, ** $p = 0.001-0.05$, *** $p < 0.0001$ versus control; paired t -test; Dunnett's Multiple Comparison Test; $n = 3$. Scale bars: 20 μm .

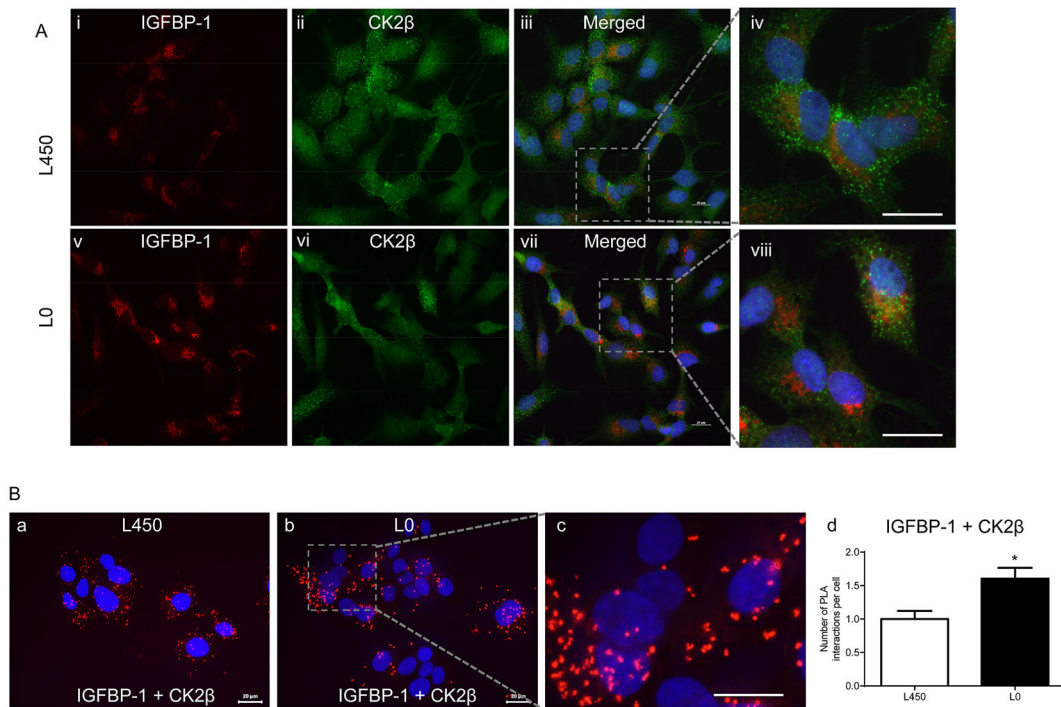


Fig. 6. L0 mediates IGFBP-1 interaction with CK2β.

HepG2 cells were cultured in L450 or L0 media and (A) immunostained to visualize (i, v) IGFBP-1 (red) with (ii, vi) CK2β (green). (iii, vii) Merged images demonstrate co-localization of PKCα and CK2β. (iv, viii) Region of interest within merged channel images. (B) Proximity ligation assay (PLA) for PKCα and CK2β in (a) L450 and (b) L0 conditions. (c) Region of interest of proximity interactions between PKCα and CK2β in L0 conditions. (d) Number of PLA signals (red dots) per cell for PKCα and CK2β proximity reactions in HepG2 cells cultured in L450 and L0 media. Values are displayed as mean + SEM. * $p < 0.05$, ** $p = 0.001-0.05$, *** $p < 0.0001$ versus control; paired t -test; Dunnet's Multiple Comparison Test; $n = 3$. Scale bars: 20 μm .

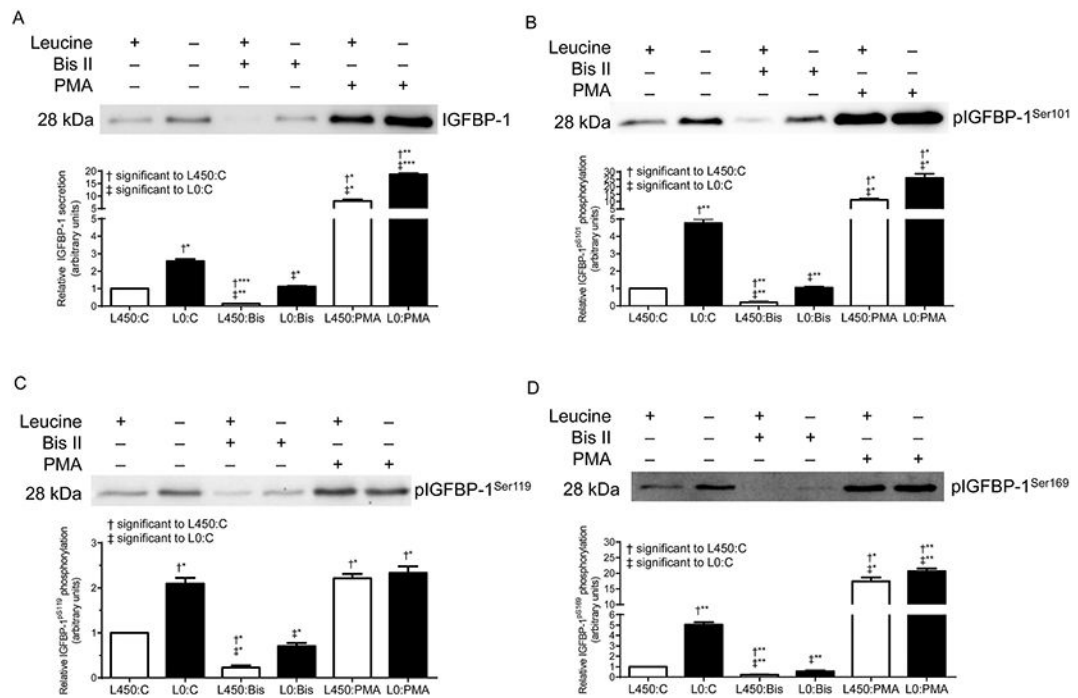


Fig. 7. PKC mediates IGFBP-1 phosphorylation.

HepG2 cells were treated with Bis II (7.5 μ M) and PMA (100 nM) and cultured with (L450) and without (L0) leucine. Representative western blots of HepG2 CM indicating (A) total IGFBP-1 and IGFBP-1 phosphorylation at (B) Ser101, (C) Ser119 and (D) Ser169. Values are displayed as mean + SEM. * $p < 0.05$, ** $p = 0.001-0.05$, *** $p < 0.0001$ versus control; One-way analysis of variance; Dunnet's Multiple Comparison Test; $n = 3$.

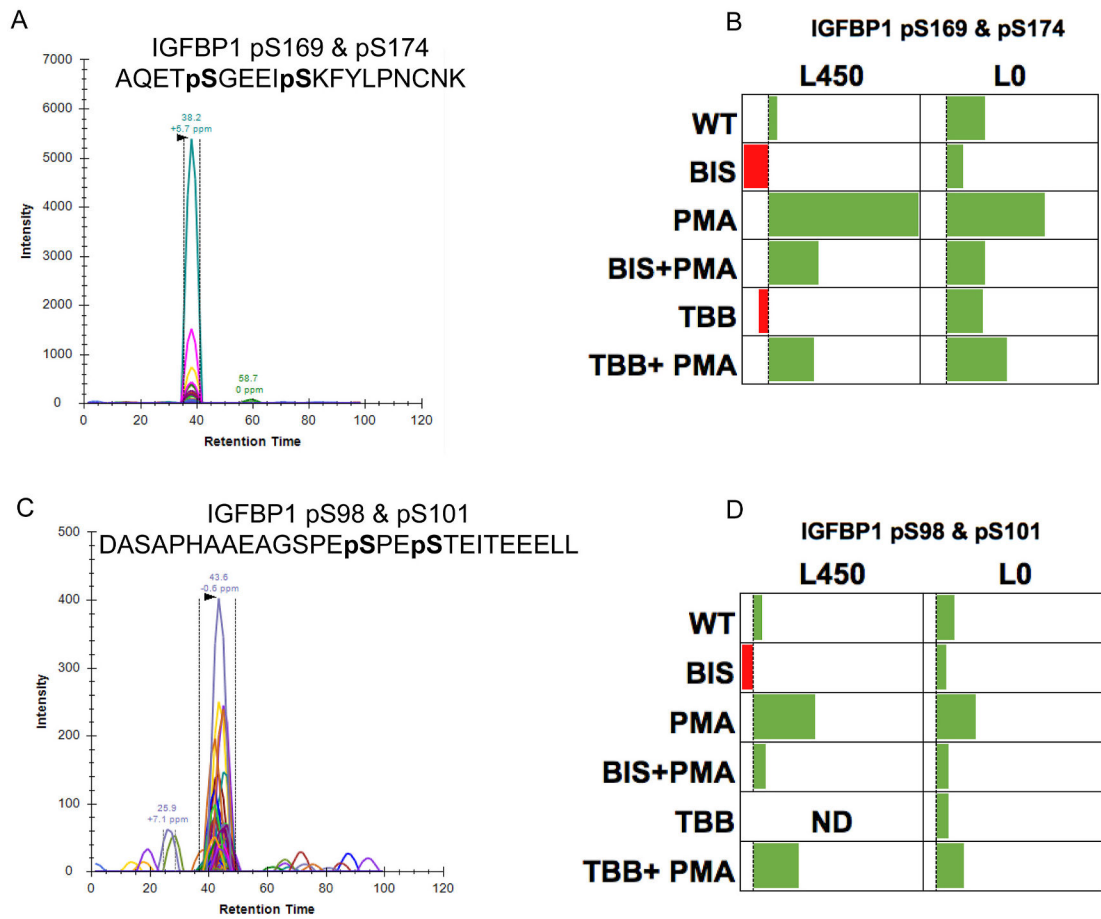


Fig. 8. Relative IGFBP-1 phosphorylation detected by PRM-MS.

Chromatogram depiction of transitions used for the discovery and detection of dual phosphorylation at (A) IGFBP-1 at Ser169/Ser174 and (B) IGFBP-1 at Ser98/Ser101 sites. Colored traces represent the detection and specificity of each transition ion. (C) Horizontal bar graphs show relative phosphorylation levels of IGFBP-1 combined phosphorylation at Ser169 + Ser174 and Ser98 + Ser101 dually phosphorylated peptide, as determined from total peak intensities of transition ions from PRM MS. Bars show relative positive (green) and negative (red) fold-change.

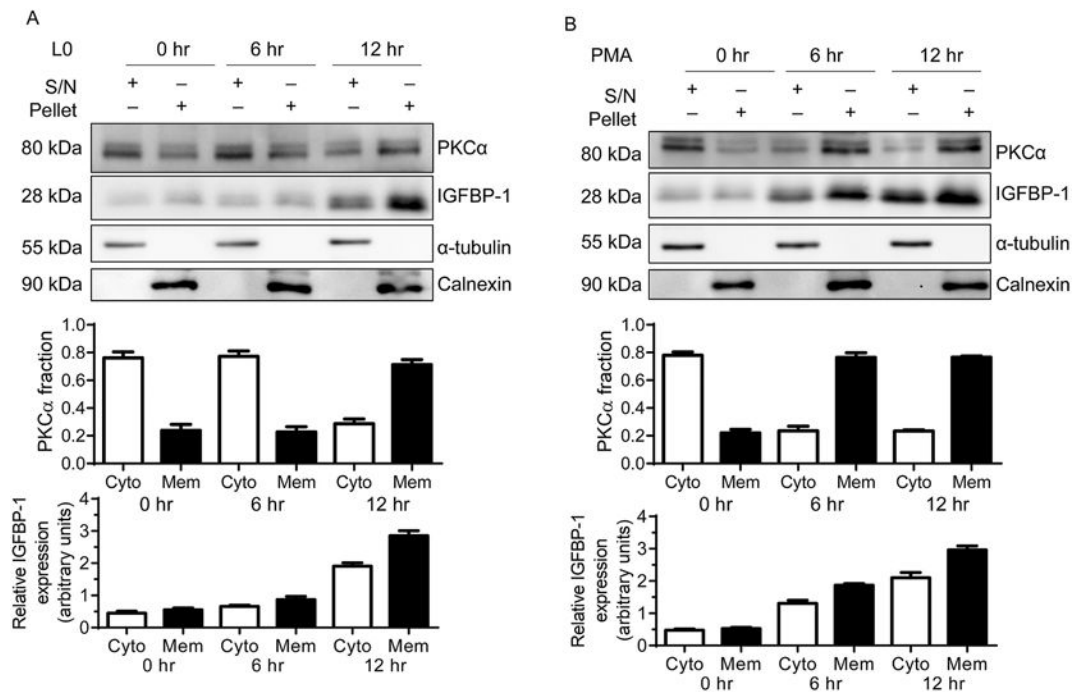


Fig. 9. Induction of IGFBP-1 expression is correlated with PKC α translocation.

HepG2 cells were deprived of leucine (L0) or treated with PMA in a time dependent manner and subcellularly fractionated by differential centrifugation to yield enriched cytosolic (S/N) and enriched membrane (pellet) fractions. **(A)** Western immunoblot of fractionated time course treated L0-cultured HepG2 cells for PKC α and IGFBP-1. **(B)** Western immunoblot of fractionated time course PMA treated HepG2 cells for PKC α and IGFBP-1.

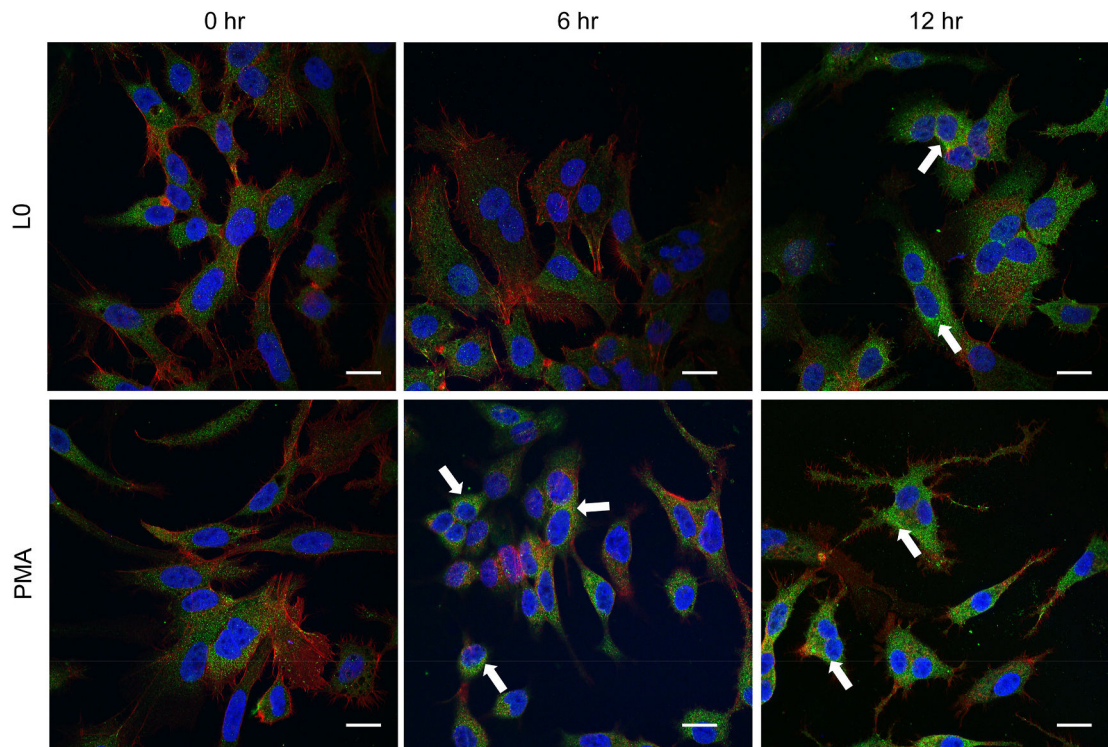


Fig. 10. Translocation of PKC α under leucine deprivation and pharmacological activation is time dependent.

Dual immunofluorescence of PKC α (green) and F-actin stain phalloidin (red) with nuclear DAPI staining (blue) demonstrate translocation of PKC α with L0 and PMA treatments.

Arrows represent areas of high density PKC α staining not present in the controls. Cell morphology changes with PMA treatment but not with L0 treatment. Scale bars: 20 μ m.

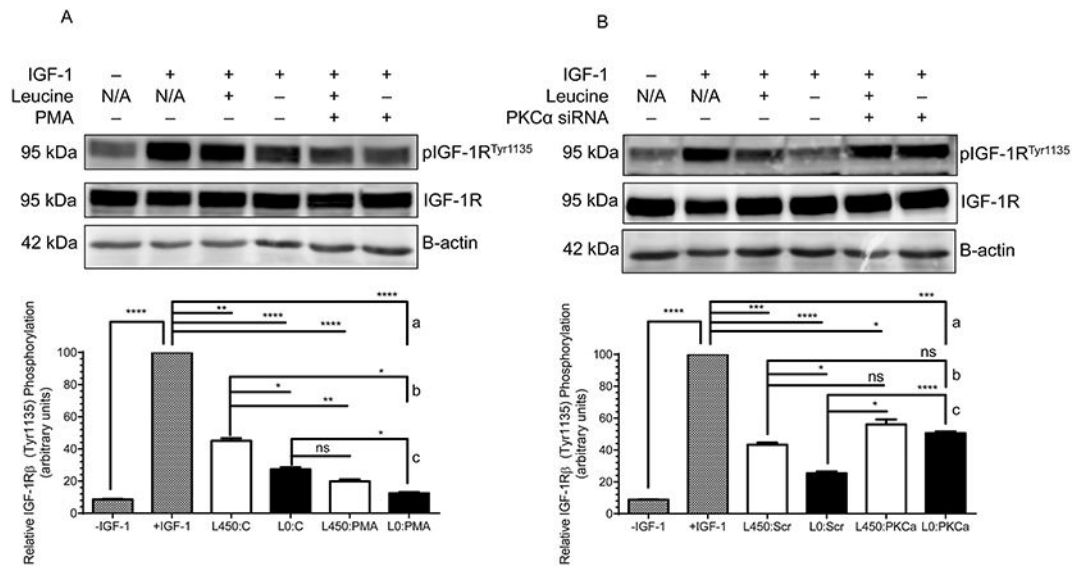


Fig. 11. PKC α mediates IGFBP-1 phosphorylation and functionally affects IGF-1R β autophosphorylation.

Representative Western blots demonstrating the effect of equal amounts of total IGFBP-1 secreted by HepG2 cells bound with IGF-I and incubated with P6 cells to induce IGF-1R β autophosphorylation. **(A)** Equal amounts of total IGFBP-1 from L450, L0, L450+PMA and L0+PMA treatments. Increased abundance of hyperphosphorylated IGFBP-1 species due to L0, PMA or combined L0+PMA treatments significantly decreased IGF-1R activation compared with control (L450). **(B)** Equal amounts of total IGFBP-1 from L450, L0, L450+PKC α siRNA and L0+PKC α siRNA treatments. Decreased abundance of hyperphosphorylated IGFBP-1 species due to PKC α silencing in L450 and L0 significantly increased IGF-1R activation compared with control (L450). Equal amounts of P6 cell lysate (40 μ g) were used on Western blot to detect IGF-1R β (Tyr1135) autophosphorylation. Values are displayed as mean + SEM. * $p < 0.05$, ** $p = 0.001-0.05$, *** $p < 0.0001$ versus control; One-way analysis of variance; Dunnet's Multiple Comparison Test; $n = 3$. Significance vs + IGF-I positive control (a). Significance vs basal control (L450:C; L450:Scr) (b). Significance vs leucine deprivation (L0:C, L0:Scr) (c).

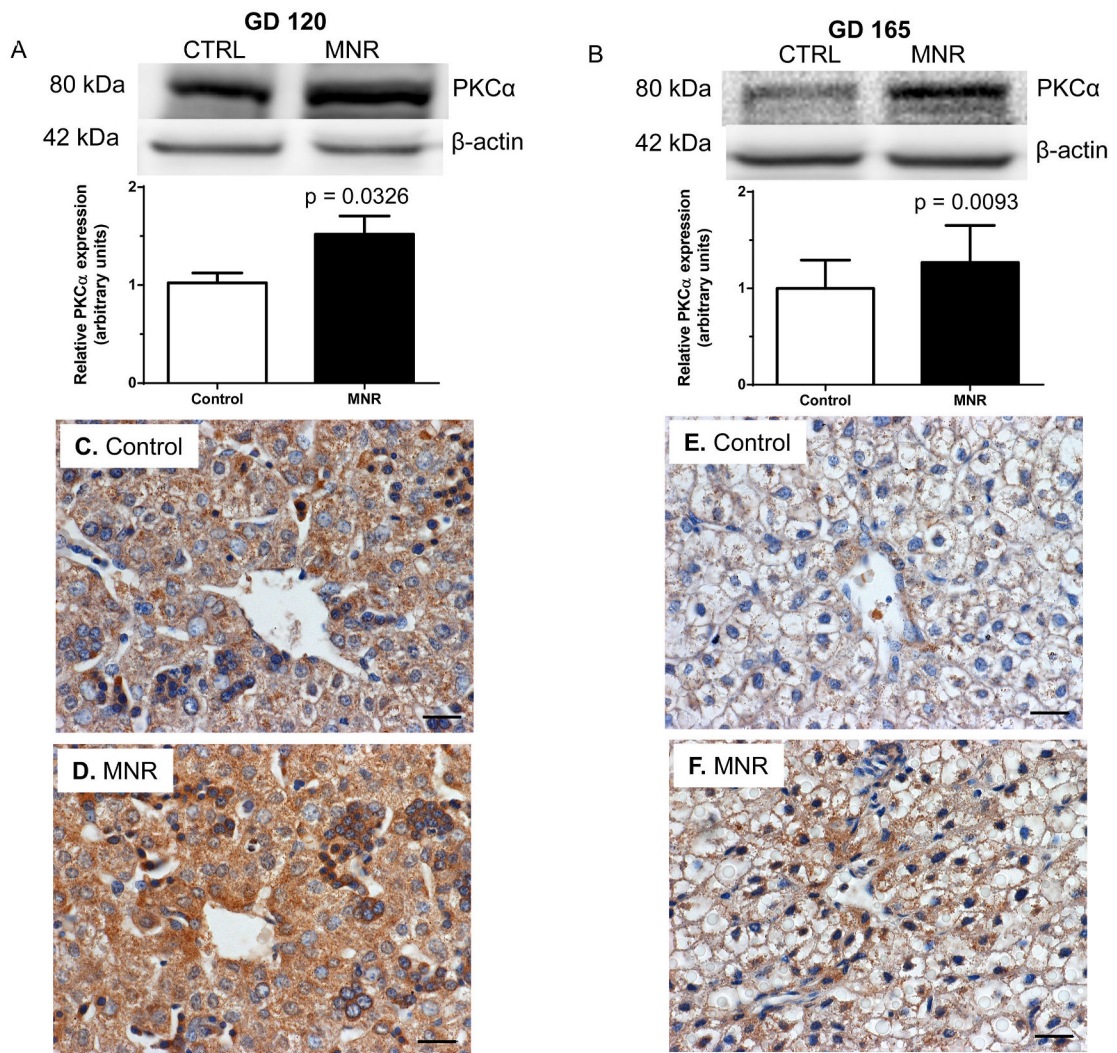



Fig. 12. PKC α expression is increased in MNR baboon fetal liver tissue at GD 120 and GD 165. Representative western blot and quantitation for PKC α expression in baboon fetal liver tissue at (A) GD 120 and (B) GD 165. Immunohistochemistry (IHC) for PKC α in sectioned baboon fetal liver tissue at GD 120 (C, D) and GD 165 (E, F). Control and MNR liver tissue sections were fixed on the same slide and immunostained against PKC α and the nucleus counterstained with hematoxylin. All IHC images are 40x. Scale bars are 20 μ m. Values are displayed as mean + SEM. One-way analysis of variance; Dunnet's Multiple Comparison Test; n = 19 (GD 120), n = 24 (GD 165).

Table 1
Detection of PKC α peptides with shared homology among conventional PKC isoforms.

IGFBP-1 and CK2 β immunoprecipitation from L0 cultured HepG2 cells co-immunoprecipitated homologous cPKC and PKC α specific peptides detected by PRM-MS.

Peptide number	ID	Sequence	cPKC Homology
1		T.DFIWGFQKQGFQCVCCFWHK.R [54, 75]	PKC α + PKC β + PKC β II
2		K.RCHEFVTFSCPGA.D [76, 88]	PKC α + PKC β + PKC β II
3		K.IHTYGSPTFCDHCGSLYGLJHQMK.C [105, 130]	PKC α
4		C.DHCGSLYGLJHQMK.C.D [115, 131]	PKC α
5		C.DMINVHKQCVINVPCLCGM.D [135, 152]	PKC α
6		K.QCVINVPCLCGMDHTEK.R [141, 157]	PKC α
7		K.TIRSTLNQWNESFTFK.L [213, 229]	PKC α
8		R.STLNQWNESFTFK.L.P [216, 231]	PKC α
9		N.DFMGSLSEGVSELMKMPASGWY.K.L [253, 275]	PKC α
10		K.MPASGWYKLLNQEEGEYYNVPIPEG.D [268, 292]	PKC α
11		K.LLNQEEGEYYNVPIPEG.D [276, 292]	PKC α
12		K.PPFLTQLHSCFQTVDR.L [396, 411]	PKC α
13		R.LYFVMEYVNGGDLMYHIQQVQVK.F [412, 433]	PKC α
14		K.FKEPQAVFYAAEISIGLFLFLHK.R [434, 455]	PKC α

Peptide number	ID	Sequence	cPKC Homology
15		P.DYIAPEIAYQPYGK.S [502, 516]	PKC α + PKC β + PKC β II + PKC γ

Author Manuscript

Author Manuscript

Author Manuscript

Author Manuscript